

# Laser induced Temperature jump

IR pulse heats the solvent

( Raman shifted YAG to  $1.9 \mu$  for  $D_2O$ )

Probe heated spot with tunable IR laser

(Pb-salt diode, FTIR experiments proposed)

Fast MCT needed for ns response

Repetition rate limited by cooling back initial state

Analysis is relaxation kinetics,  $k_{rel} = k_f + k_r$

Signal average thousands of shots,

single frequency (diode laser) normal method

# Callender/Dyer general T-jump setup

Fluorescence use cavity doubled, lots cw power

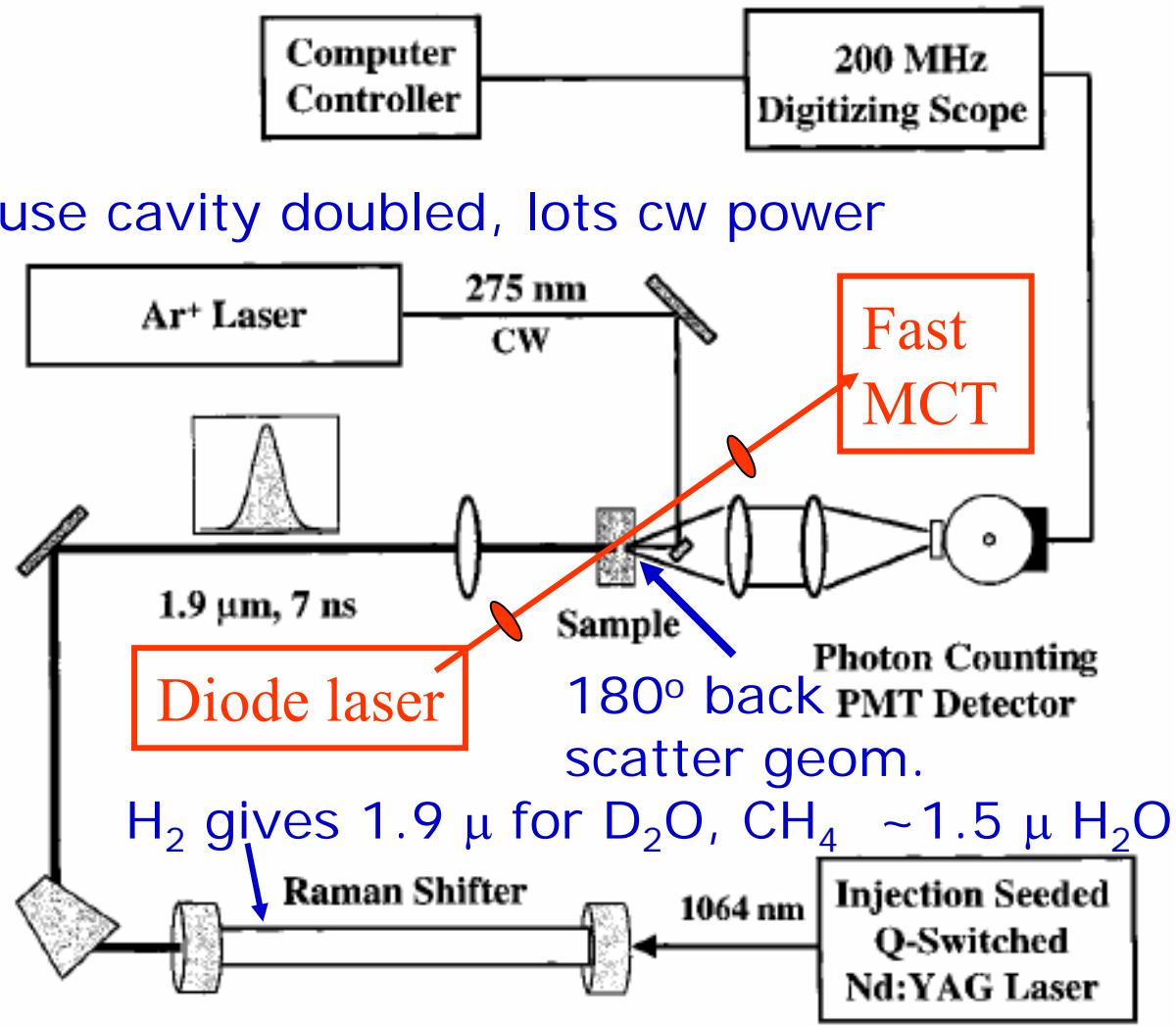


FIGURE 2: Schematic of the fluorescence *T*-jump spectrometer. See the text for details.

Generic design for T-jump, IR diode laser detection transmit to MCT

# Brian Nolan\*, Edward Gooding\*, Sapna Sharma\*, Martin Volk\*

Chemistry and Biochemistry, Swarthmore College \*Surface Science Research Centre, University of Liverpool

Temperature-jump experiments used direct D<sub>2</sub>O excitation via a pulsed 1.9 μm pump and a CW probe with fast detection and a digitizing scope

Variant of Dyer design uses difference frequency generation, shorter pulse smaller ΔT

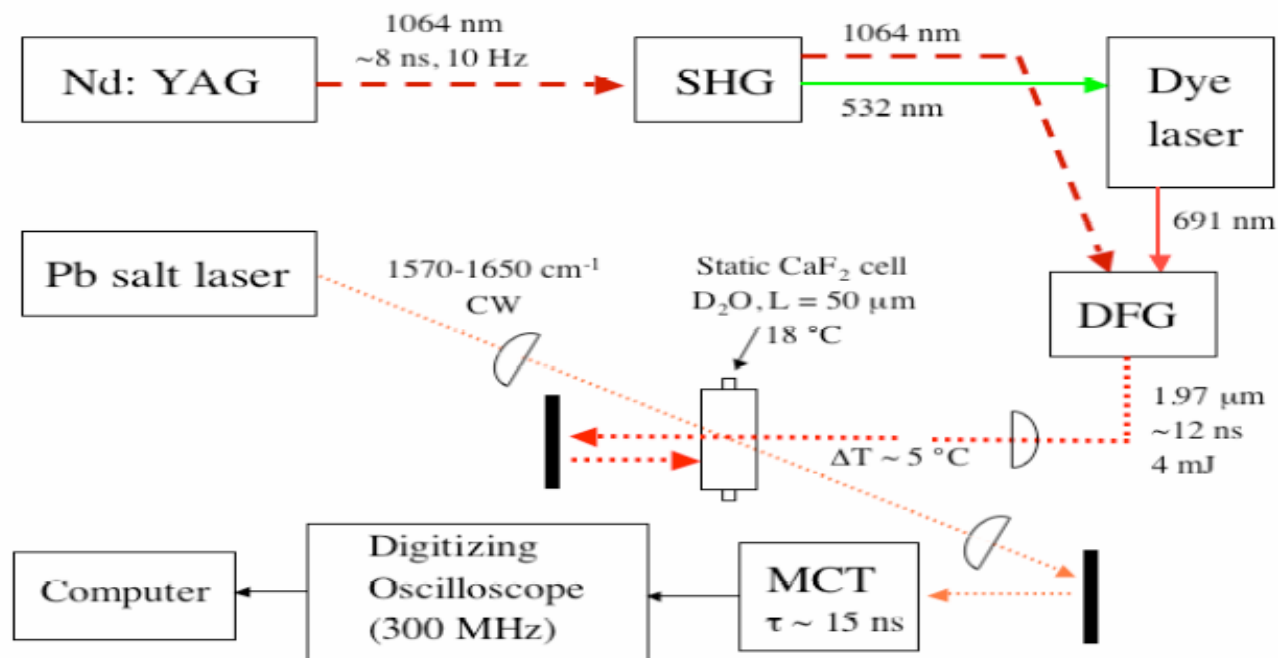


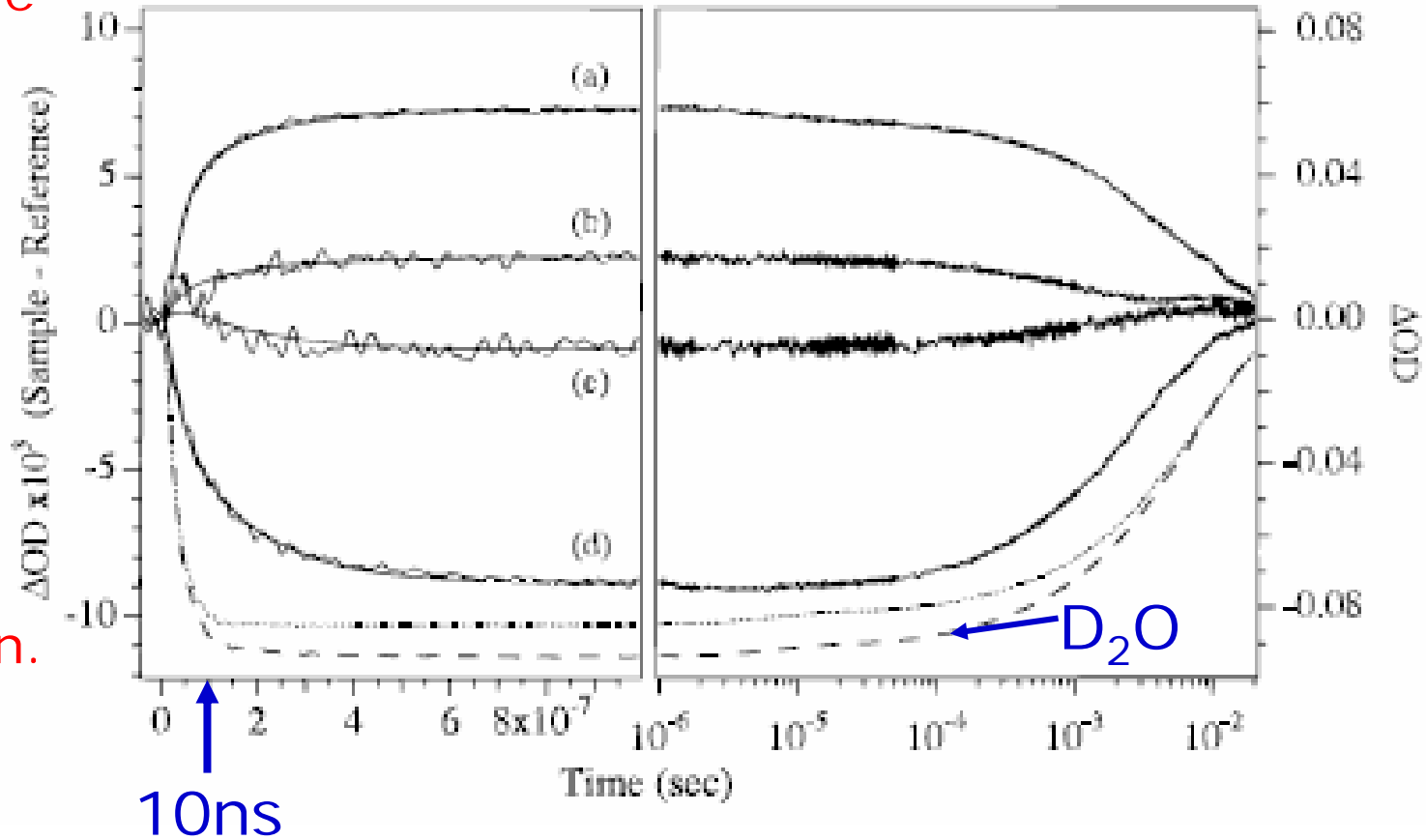
**Fig. 2.** The pump beam (heavy lines) at 1.9 microns directly pumps a D<sub>2</sub>O absorption band. The excitation is converted to a temperature rise of about 5 °C on a subnanosecond timescale. We monitor the change in absorbance of the (CW) probe beam in the amide I' region with a fast digitizing oscilloscope.

# Character of Temperature jump--timing

## Helix example

D<sub>2</sub>O - - -  
Sample .....  
Difference:  
a-1655 cm<sup>-1</sup>  
b-1644 cm<sup>-1</sup>  
c-1637 cm<sup>-1</sup>  
d-1632 cm<sup>-1</sup>

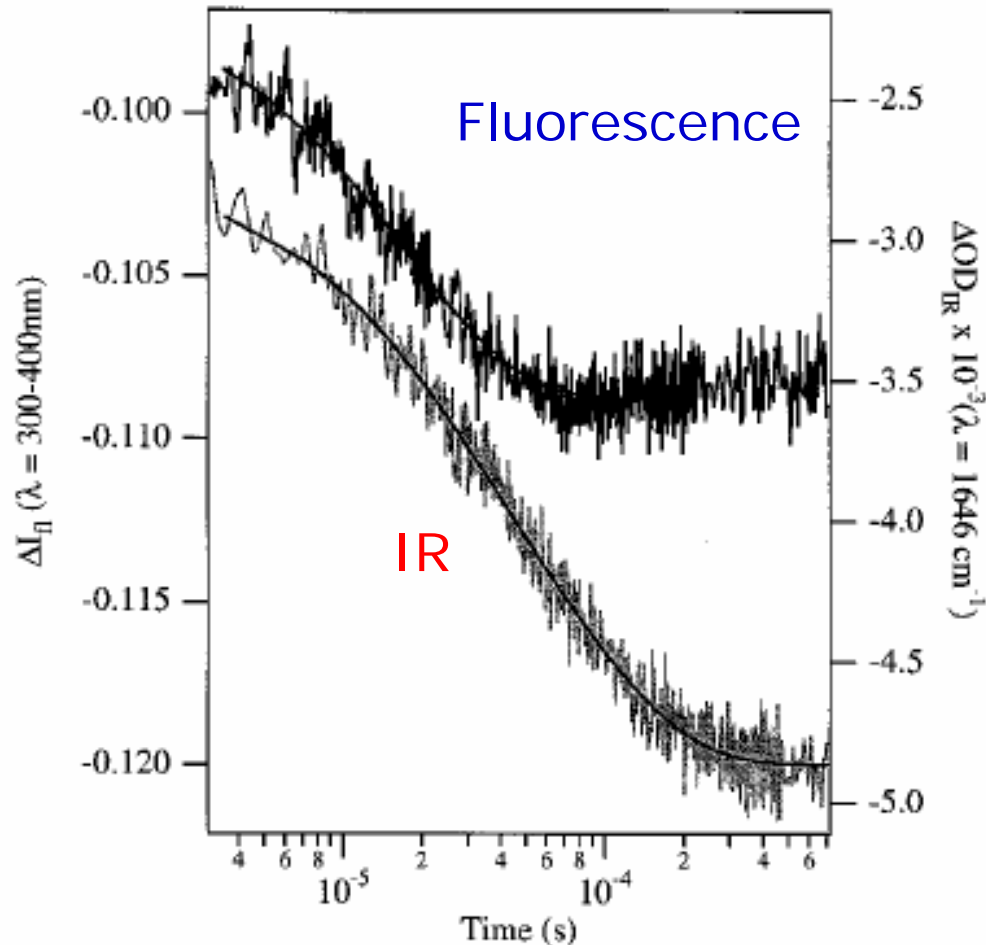
Fit to biexpon.  
<10 ns  
160+/-60 ns



Pump  $\Delta T$  at 2 $\mu\text{m}$  focus to 300 $\mu\text{m}$ , 110  $\mu\text{m}$  path use split cell  
fast (50MHz) MCT detector, avg. 9000 shots, 10 Hz

T-jump calibrated by change of D<sub>2</sub>O absorption with temperature  
3.0x10<sup>-5</sup> to 4.0x10<sup>-5</sup> (OD)/°C.  $\mu\text{m}$  for 1700 and 1632 cm<sup>-1</sup>

# Apo-Mb kinetics, T-jump Fluorescence & IR



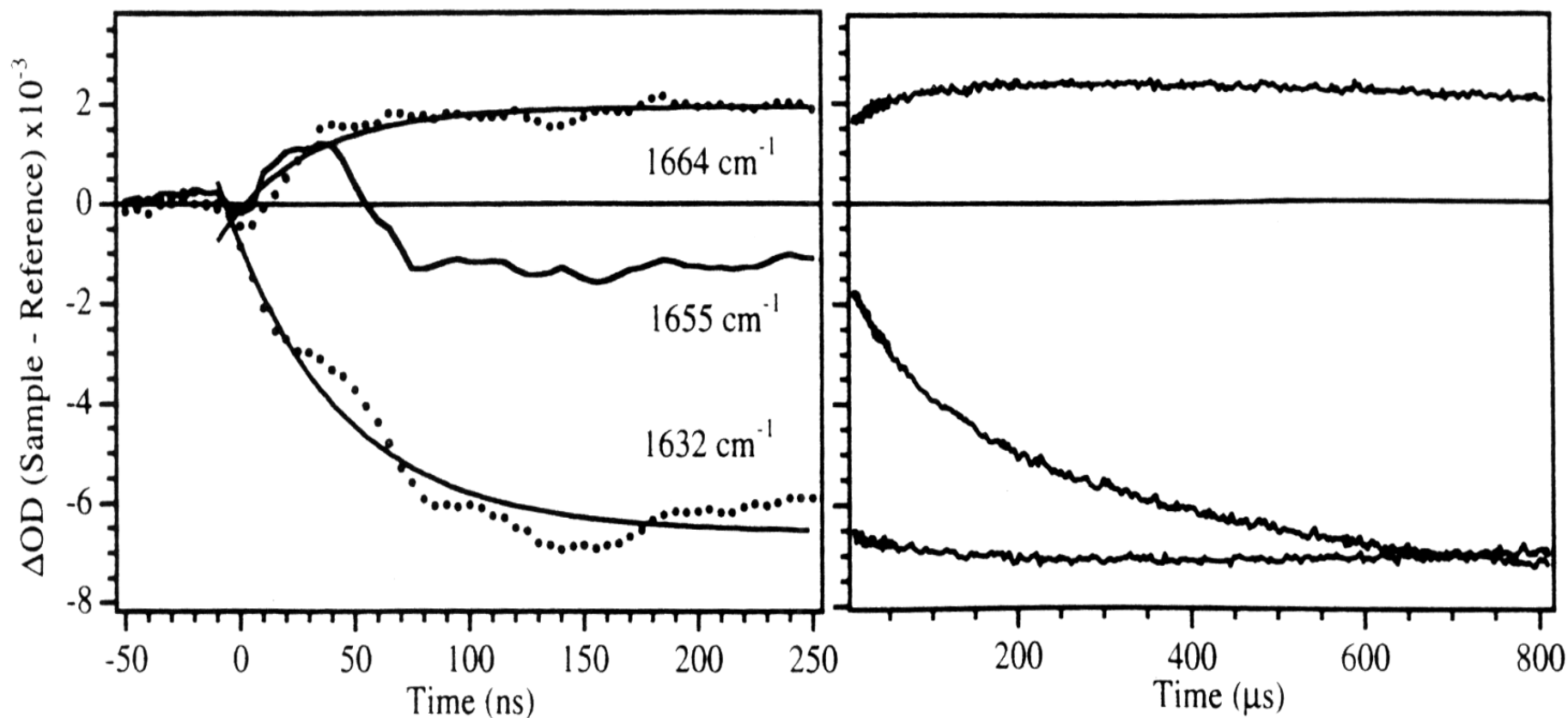
Follow different processes,  $\mu s$  response

Fluorescence – tertiary structure unfold

IR – secondary structure - helices

FIGURE 4: Fluorescence (top trace) and IR (bottom trace) kinetics traces for the E state of apoMb following a *T*-jump from 42 to 54 °C. Both samples were in 20 mM NaCl at pH\* 3.0 (D<sub>2</sub>O). The concentration of apomyoglobin used in the fluorescence studies was 2 mg/mL. The concentration used for the IR studies was 4–8 mg/mL.

# Kinetic IR response to T-jump (45-60 C) - apo Mb



Solvated helix (1632  $\text{cm}^{-1}$ ) lost very fast,  $\sim 100$  ns, as is 1664 (turns?)  
protected helices (1655  $\text{cm}^{-1}$ ) slower. Laser pulse heat water in 10's ns

# T-dependence of rates (Arrhenius)

IR-two phases

Fluorescence (+)

match fast IR (x)

Activation energy  
can be determined

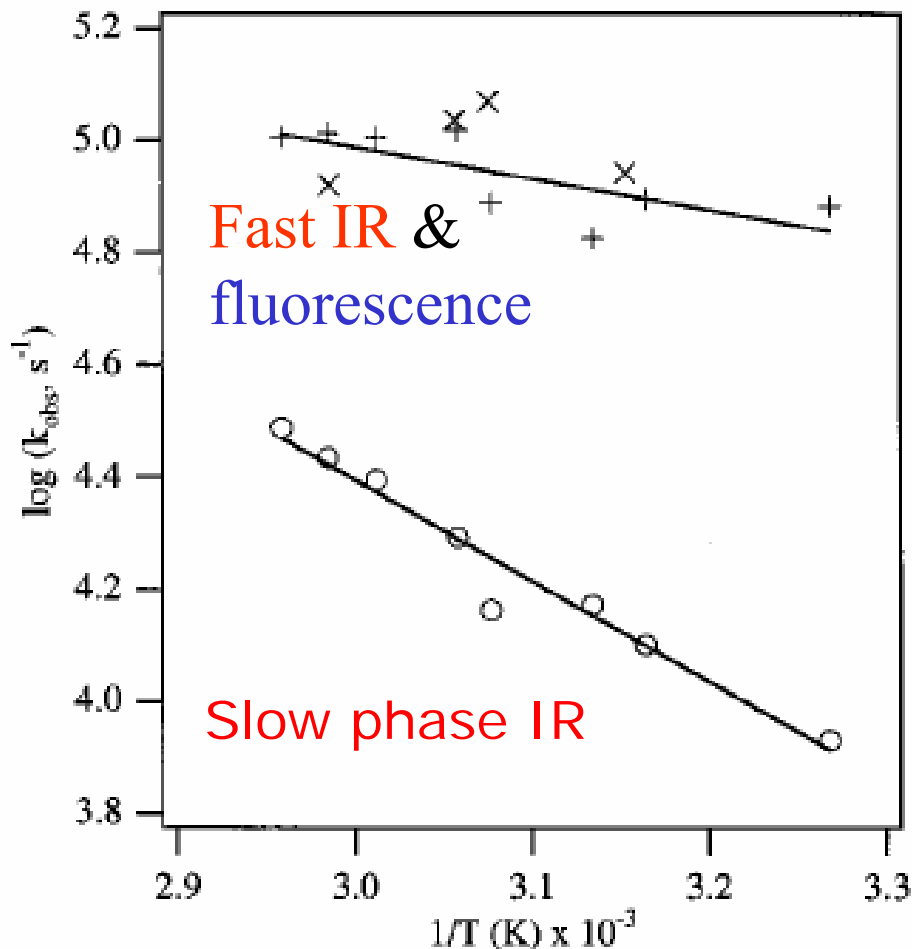


FIGURE 5: Temperature dependence of the two phases. The  $1/T$  axis represents the temperatures reached during the  $T$ -jump. The data points show the rate dependence for the fluorescence data (+), the fast phase in the IR data (x), and the slow phase in the IR data (O). A linear least-squares regression algorithm using an Arrhenius function was used to determine the best straight line fit to the data (both the emission and IR data being used in the fit). The apparent activation energies obtained from the fit are 2 and 8 kcal/mol to

# Villin head-piece – very fast folder

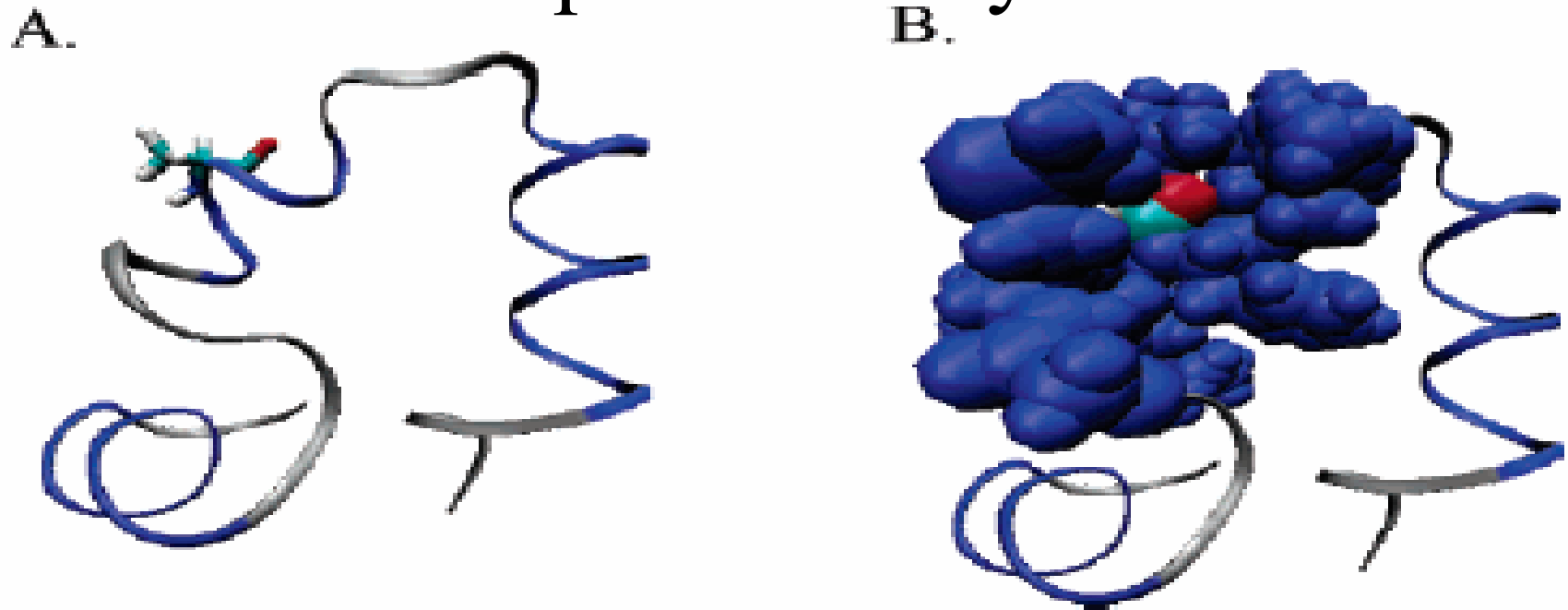


FIGURE 1: Structure of the villin headpiece subdomain (HP36) (Protein Data Bank structure 1VII) highlighting the alanine residue (A57) containing the amide  $^{13}\text{C}=\text{}^{18}\text{O}$  isotopic label (A). The four residues on either side of A57 are shown in a space-filling representation (blue) to illustrate the solvent accessibility of the carbonyl group of A57 shown in cyan (carbon atom) and red (oxygen atom) (B). The sequence of the protein is *MLSDED-FKAVFGMTRSAFANLPLWKQQNLKKEKGLF* with A57 in italics. The number of the first residue is 41 using the numbering system from previous publications. The figure was generated using the program VMD (38).



# A57 $^{13}\text{C}$ labeled Vilin Head-piece Results (IR/T-Jump)

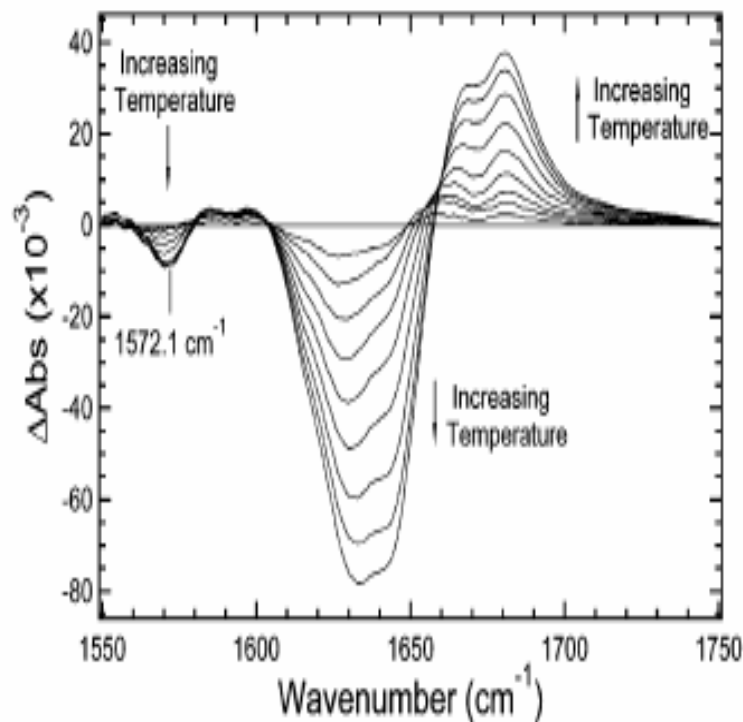


FIGURE 2: Temperature-dependent difference FTIR spectra of A57- ( $^{13}\text{C}=\text{O}$ ) HP36 from 7 °C to 86 °C in  $\sim 10$  °C increments. The difference spectra are produced by subtracting the lowest temperature absorbance spectrum from the higher temperature spectra. The peak corresponding to the carbonyl stretch of the  $^{13}\text{C}=\text{O}$  label for residue A57 appears at 1572.1  $\text{cm}^{-1}$  in the folded state.

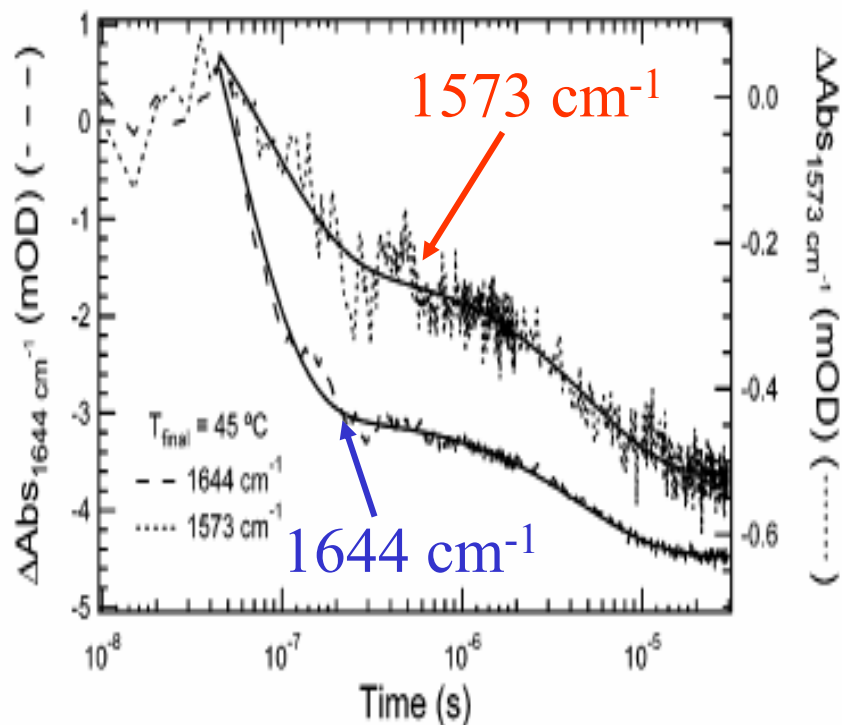


FIGURE 5: Temperature-jump relaxation kinetics monitored at 1573  $\text{cm}^{-1}$  (short dashed) and 1644  $\text{cm}^{-1}$  (long dashed) for A57( $^{13}\text{C}=\text{O}$ ) HP36 in response to a T-jump from 41 °C to 45 °C. The kinetic traces at 1573 and 1644  $\text{cm}^{-1}$  are the result of 16 000 or 10 000 laser shots, respectively. The kinetic traces are fit with a biexponential function (solid curves).

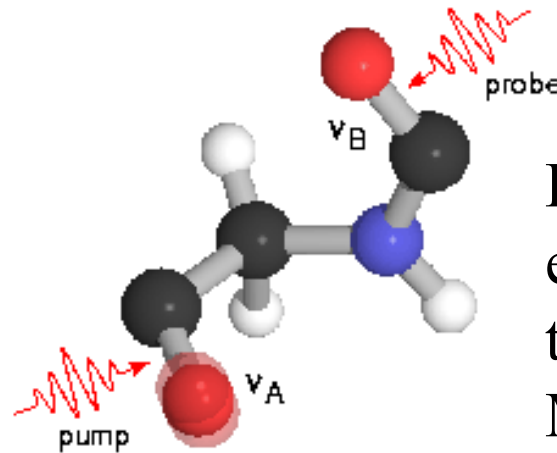
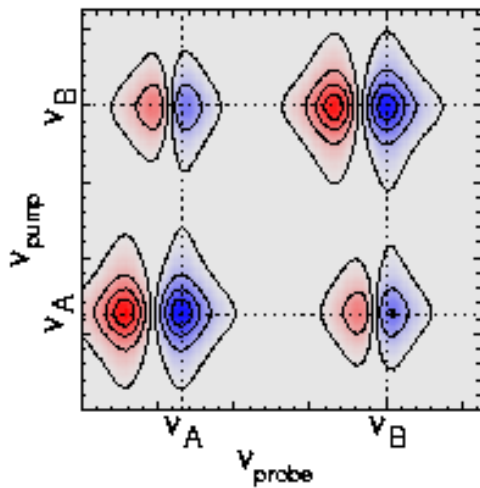
# **Advanced techniques**

**Multidimensional (2D)**

**TeraHertz (farIR)**

**Modulation Spectra (VCD)**

# 2D IR Coherence Spectra—like NMR COSY



Pump one mode, see effect on other mode through time evolution  
Modes must be anharmonic and best if resolved

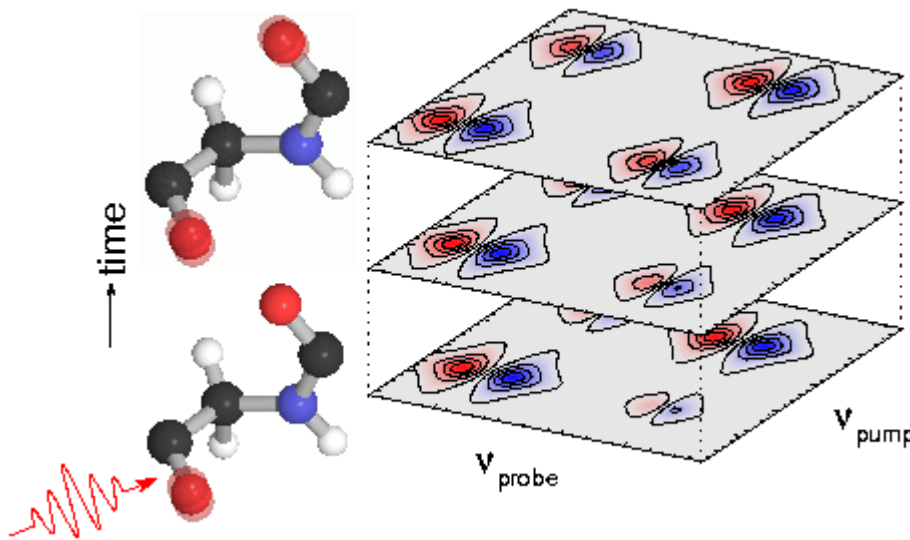


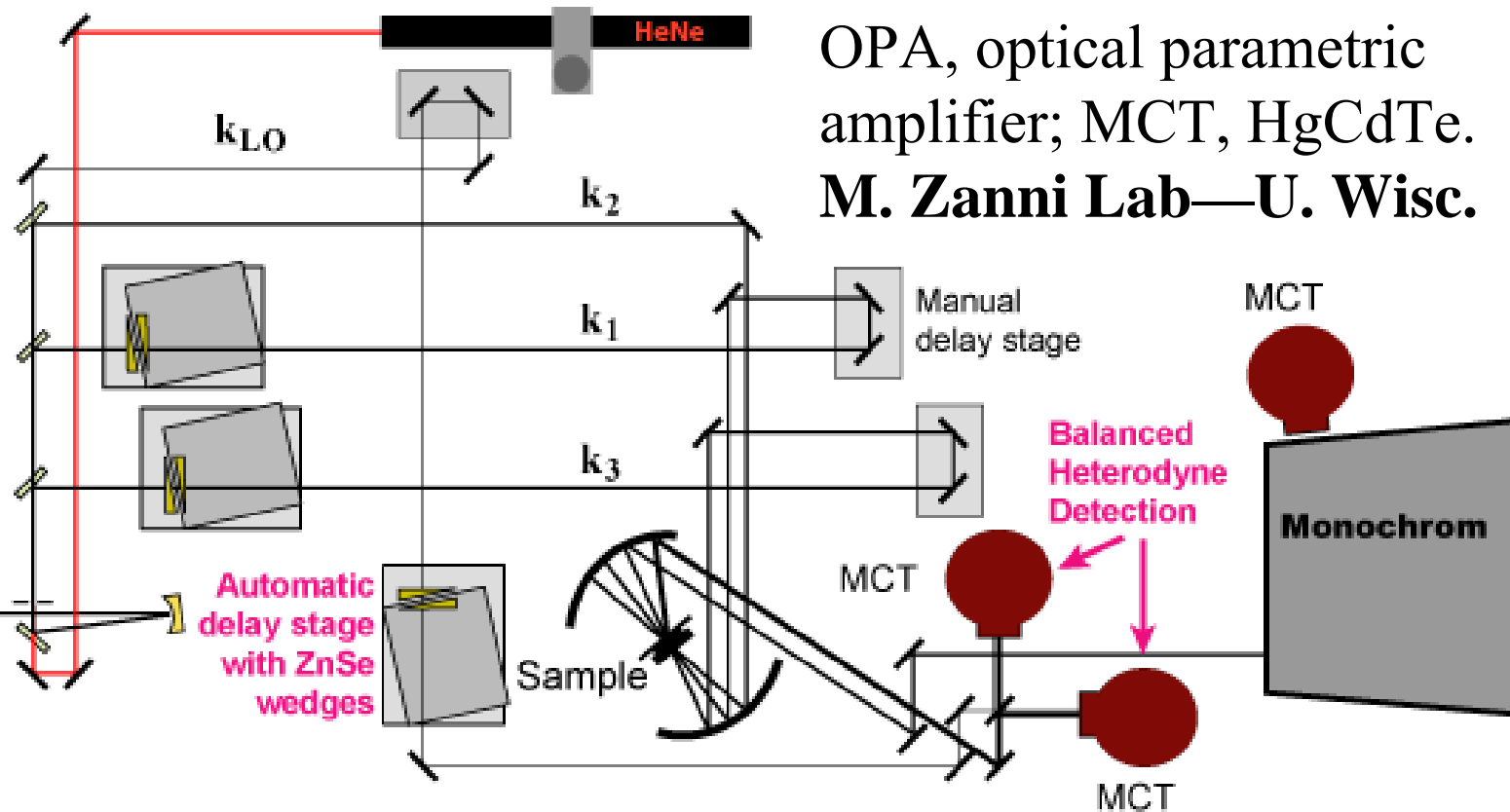
Figure from Woutersen web site

# Experimental 2D IR setup

fs laser

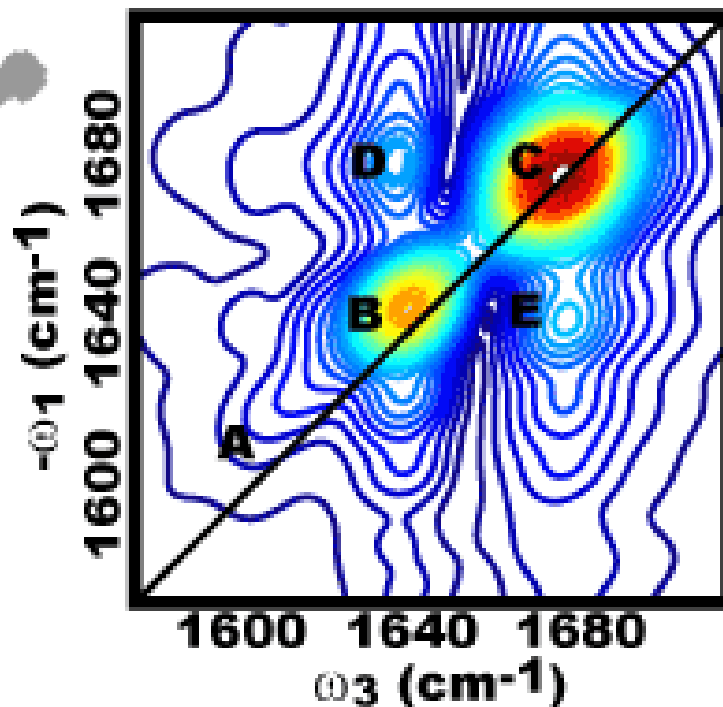
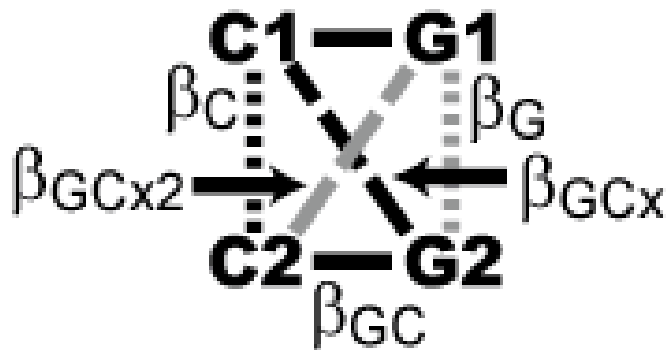
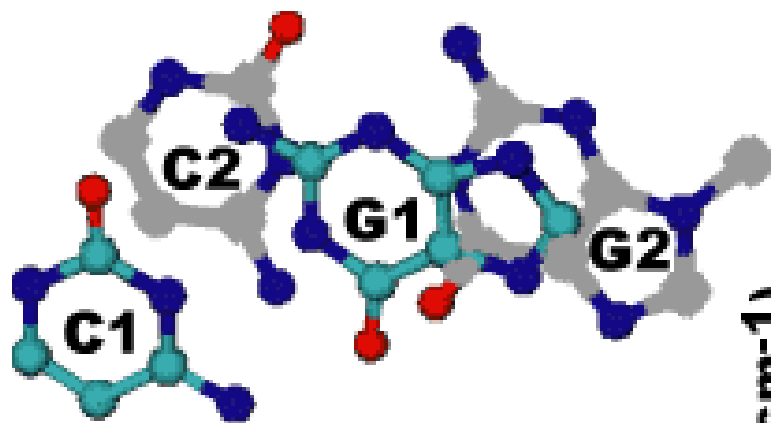
**Spectra-Physics Laser System**  
*Tsunami Evolution X Spitfire*

**OPA**  
*BBO and AgGaS<sub>2</sub>*



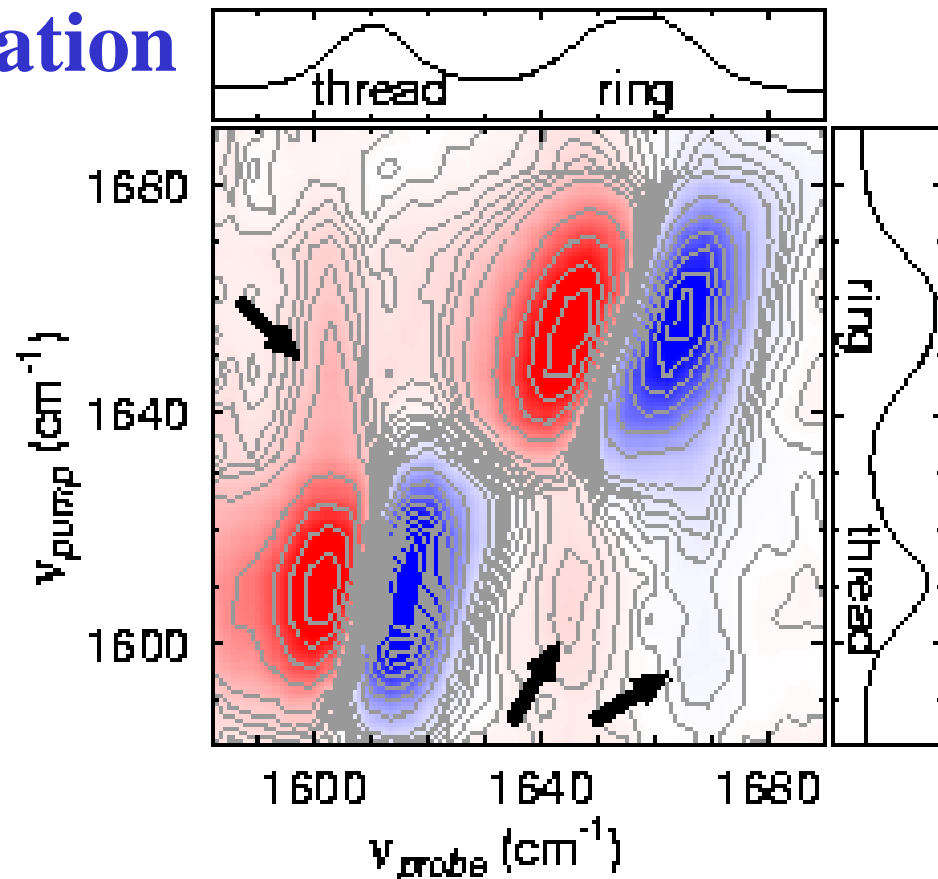
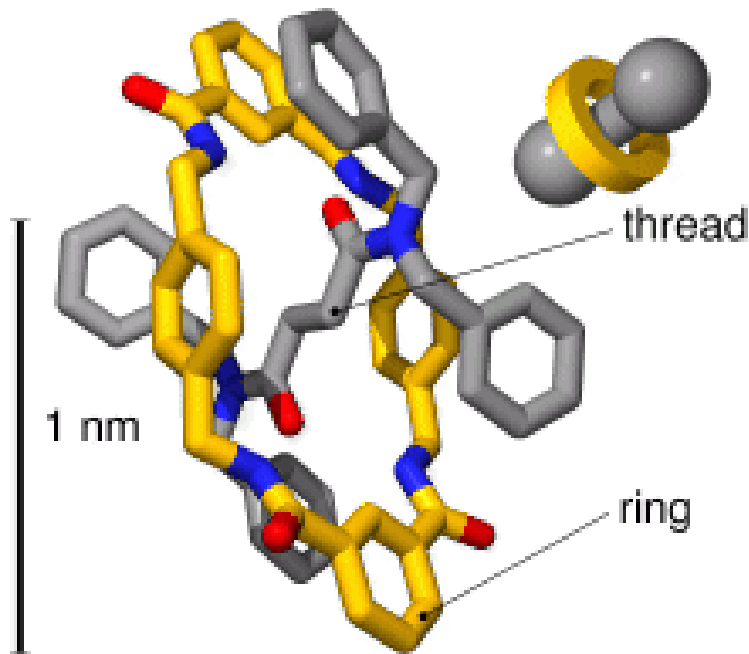
OPA, optical parametric amplifier; MCT, HgCdTe.  
**M. Zanni Lab—U. Wisc.**

2D IR uses 3 fs pulses, so 2nd excited states are measured. After heterodyning the response signal with a local oscillator pulse, 2D data set is collected and a FT along two time axes gives the 2D IR spectrum. Because overtone and combination bands are measured, 2D IR spectra exhibit cross peaks between coupled vibrational modes.



Rephasing  $\langle VVV \rangle$  2D IR spectrum of (dG5C5)<sub>2</sub> and a model of the coupling interactions for calculation the 2D IR spectrum

# 2D IR dynamic conformation In a molecular complex



Cross-peaks (indicated by arrows) reflect couplings between C=O groups. From the couplings and anisotropies, solution conformation of the ring-thread system is determined on a sub-ps time scale. Fluctuations in conformation are observed with time-delayed 2D-IR.

**Probing the structure of a rotaxane with 2D infrared spectroscopy - PNAS 2005**  
**O.F. A. Larsen, P. Bodis, W. J. Buma, J. S. Hannam, D. A. Leigh, S. Woutersen**

# Single shot 2D IR spectroscopy

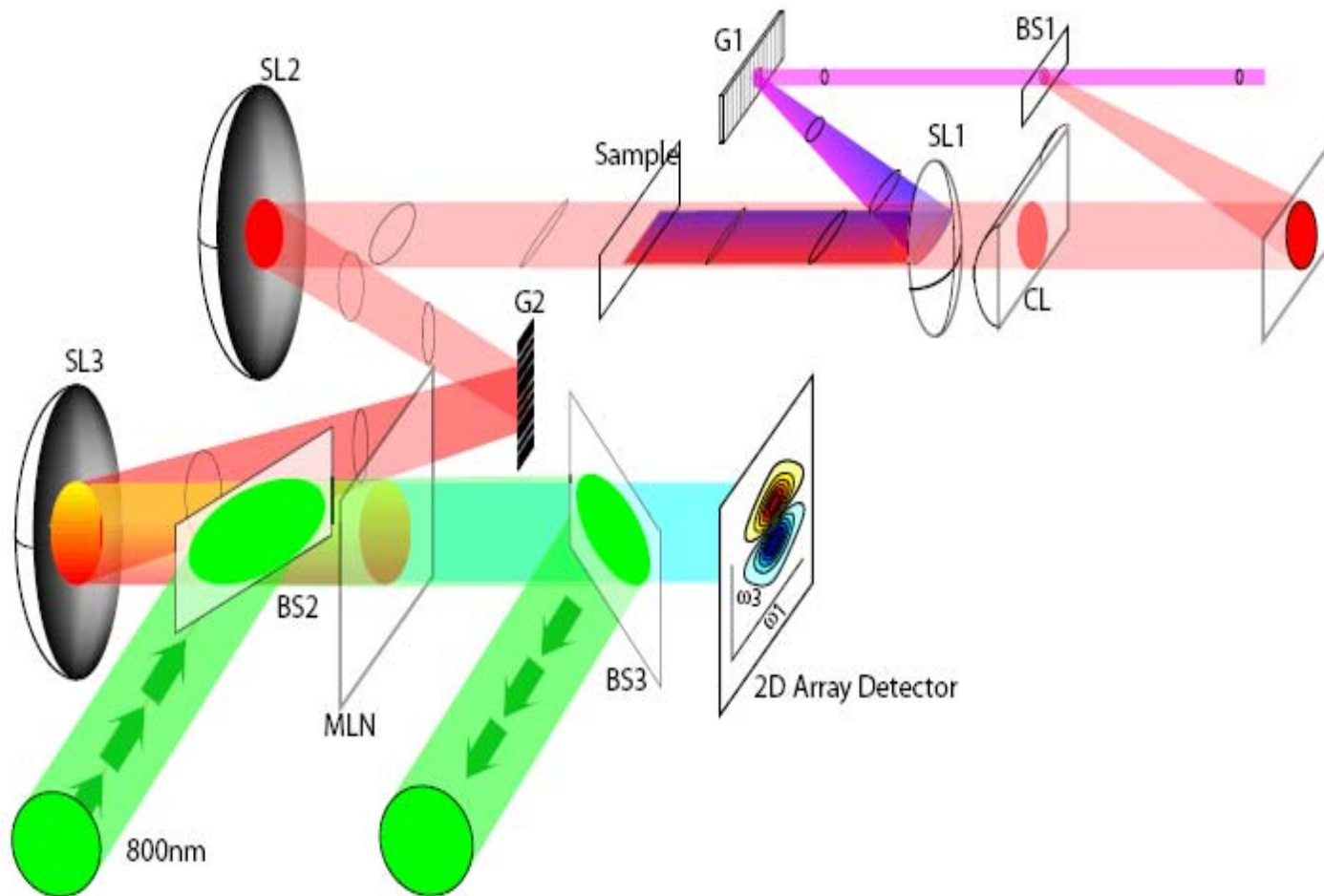


Fig. 1. 2DIR spectrometer. G is diffraction grating, SL is a spherical focusing mirror, CL is a cylindrical lens, BS is a beamsplitter, and MLN is the upconversion crystal.

Tokmakoff and co-workers, *Optics Express*, 15, 233, 2007

# Single shot 2D IR spectroscopy

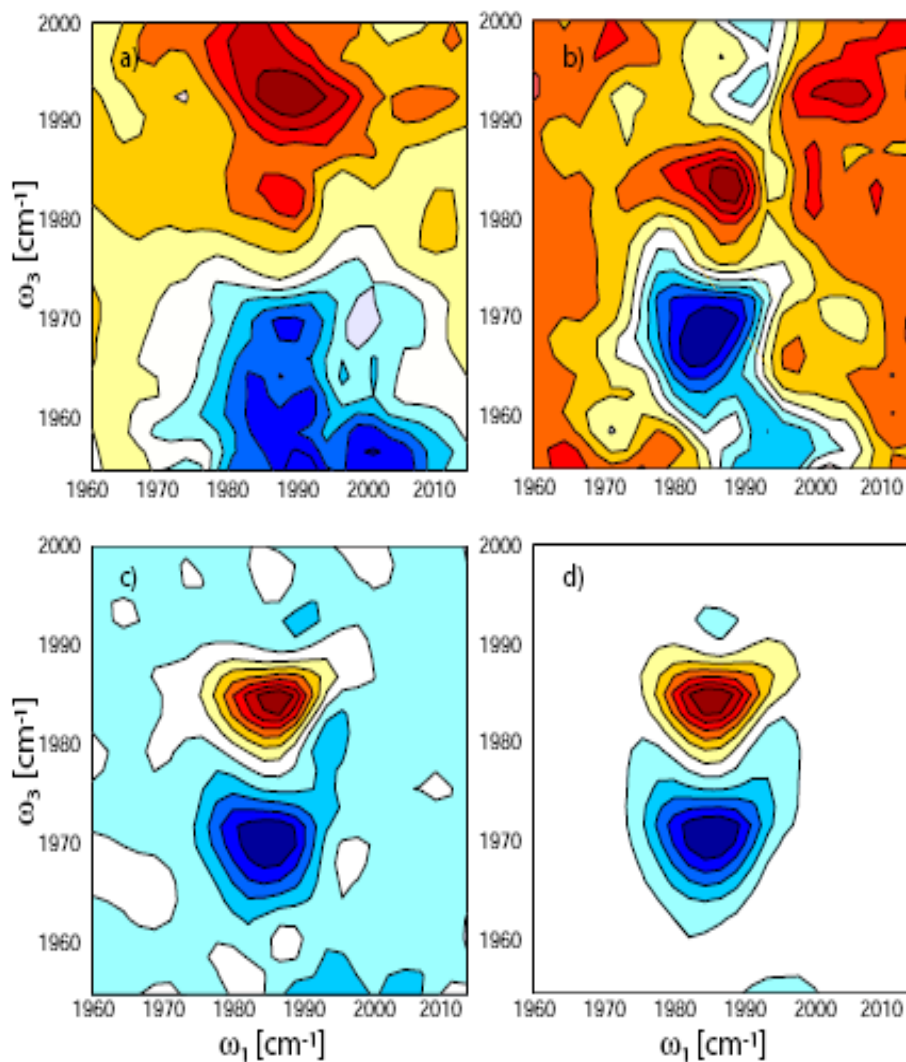


Fig. 4. Time series of 2DIR difference spectra of WHC in hexane using (a) 1 (b) 16 (c) 256 (d) and 4096 pump-probe pulses.

Tokmakoff and co-workers, *Optics Express*, 15, 233, 2007



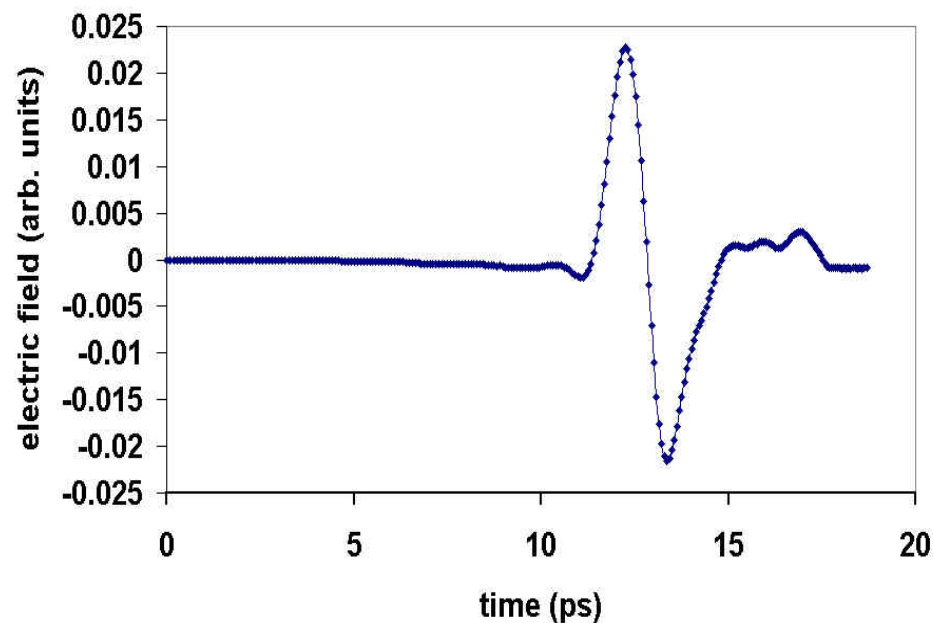
- **TeraHertz Spectroscopy**
- **The new Far-IR spectra with fs time response**

# Colgate THz Spectrometer

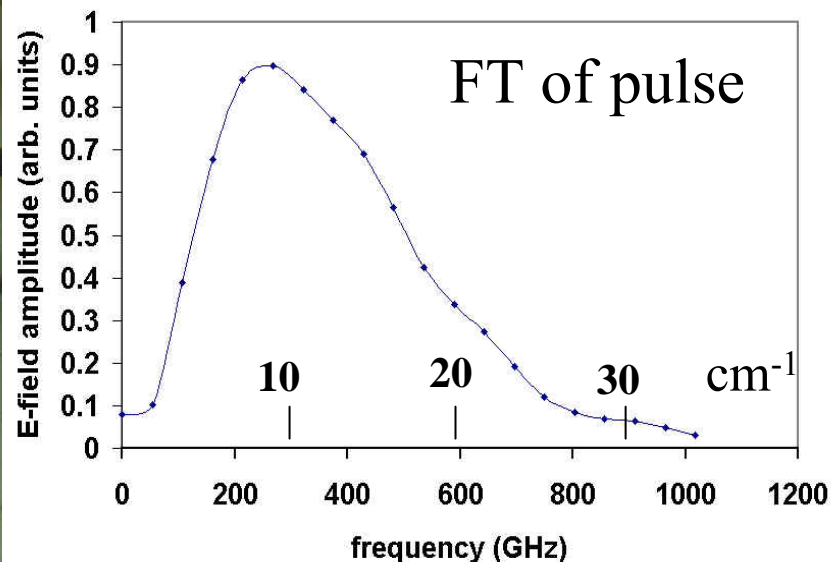
fs laser pulses hit a “THz antenna,”  
GaAs xtal. generating THz pulse

The antenna is in the brass holder  
located in the lower left. Parabolic  
mirrors focus the THz to sample  
and back to a receiver antenna.

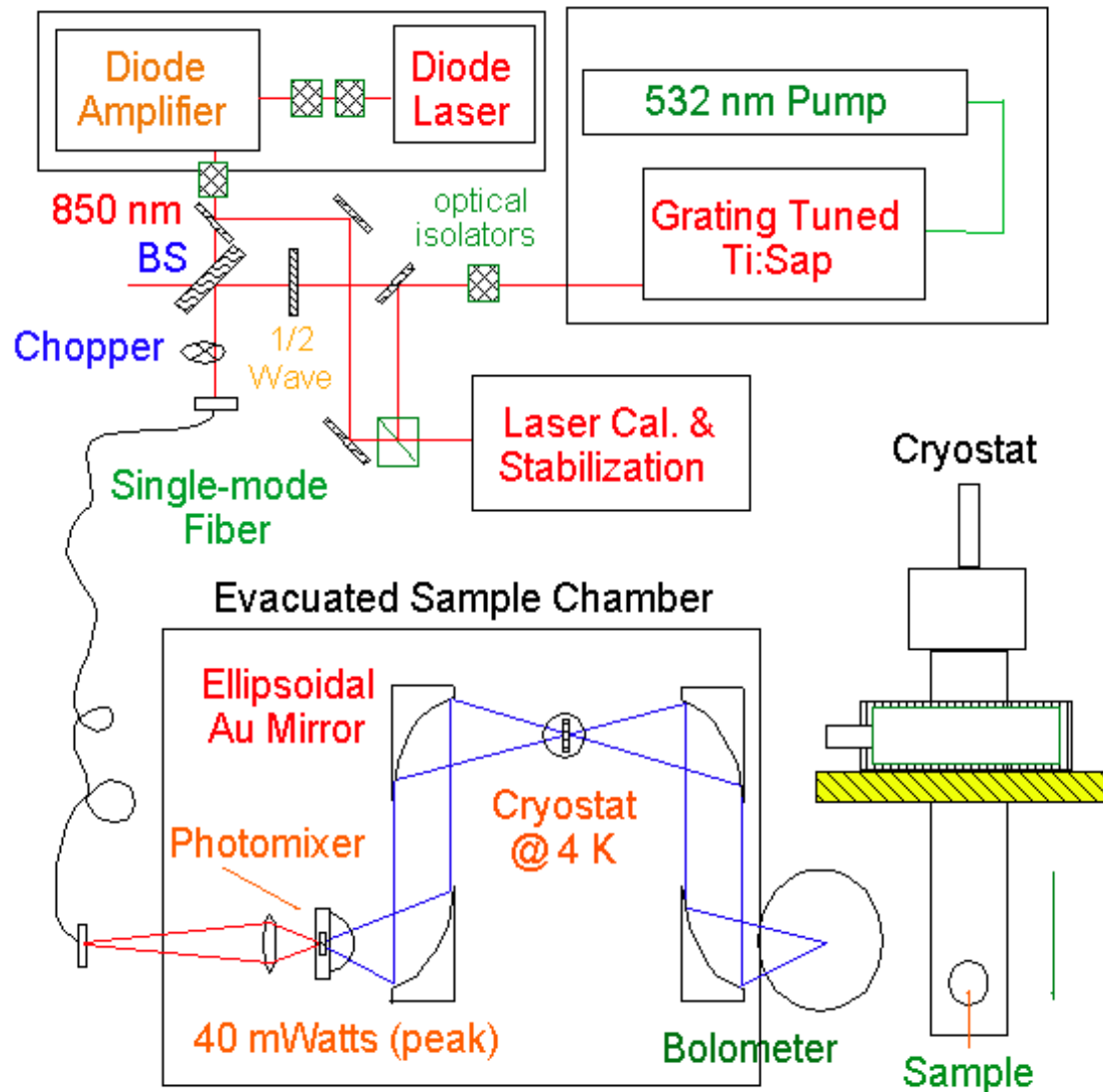
Electric field of THz pulse as a function of time



Frequency content of THz pulse

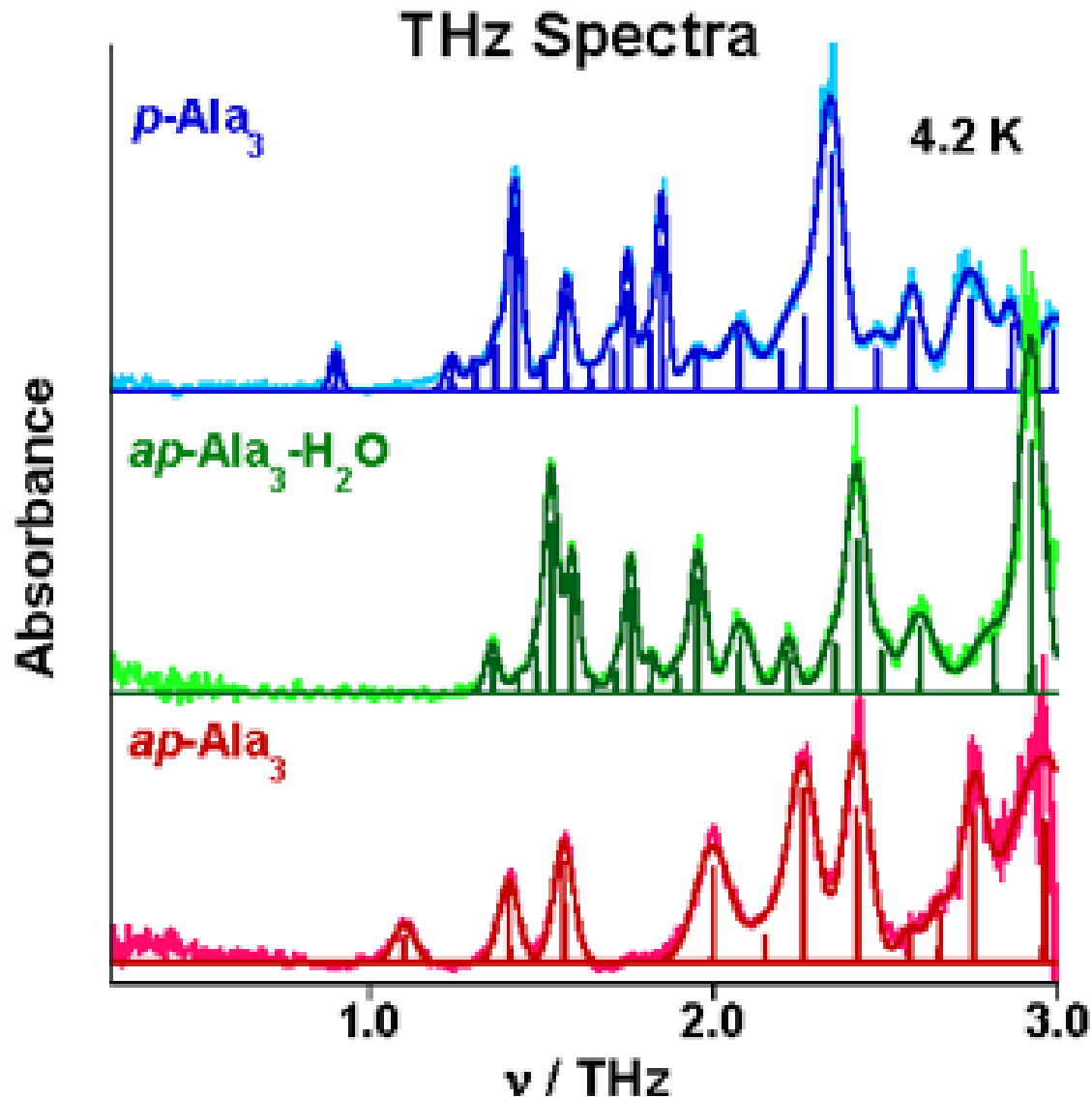


# THz Photomixer Spectrometer

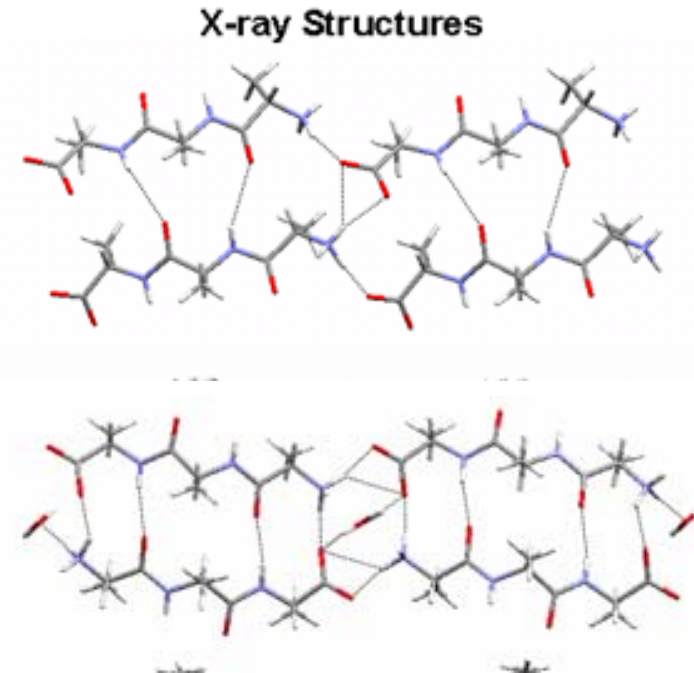


T.M. Korter and D.F. Plusquellic,  
Chem. Phys. Lett. **385** 45-51 (2004)

NIST cw THz spectrometer. The system consists of a low-temperature-grown GaAs photomixer driven at the difference frequency of two near-infrared lasers. The two lasers include a fixed frequency diode laser operating near 850 nm and ( $\Delta\nu_{\text{FWHM}} \sim 0.0001 \text{ cm}^{-1}$ ) and a standing-wave Ti:Sapphire (Ti:Sapp) laser having a resolution of ( $\Delta\nu_{\text{FWHM}} 0.04 \text{ cm}^{-1}$ ). The laser is seeded by feedback from an external grating-tuned cavity for absolute frequency stability.

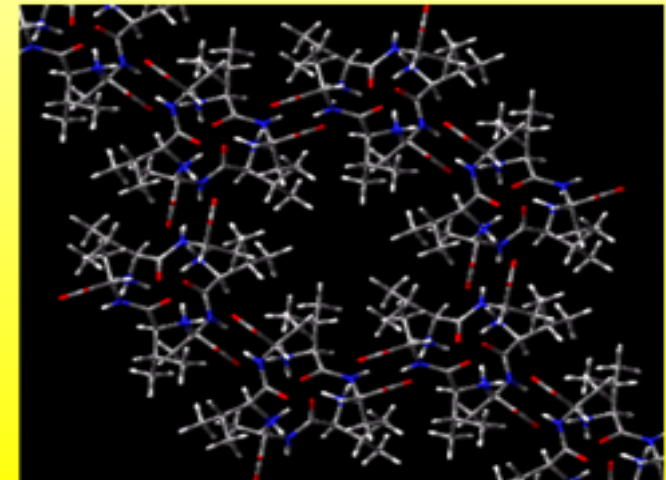
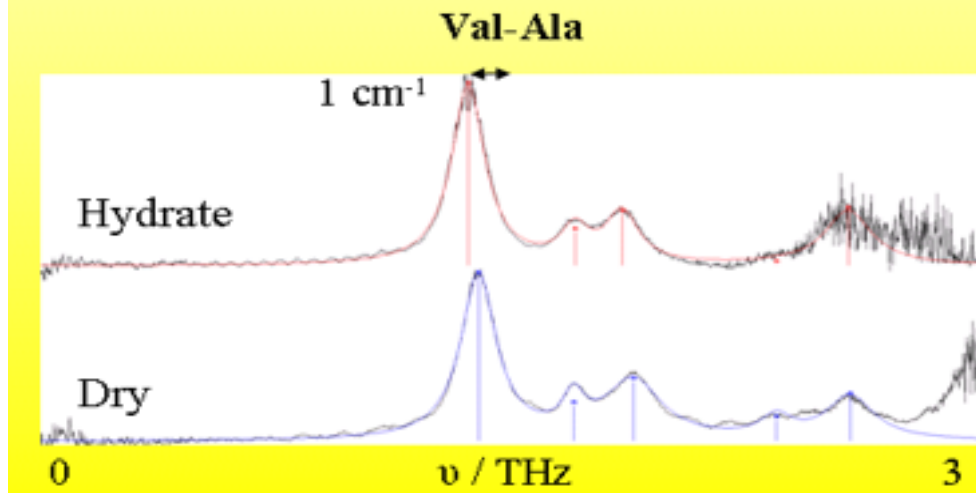
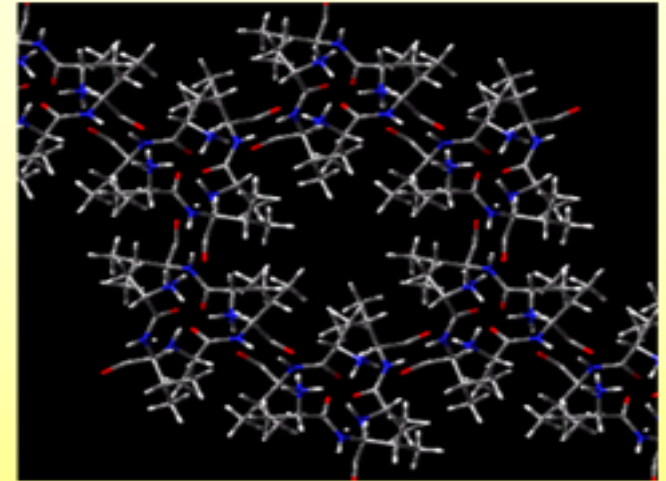
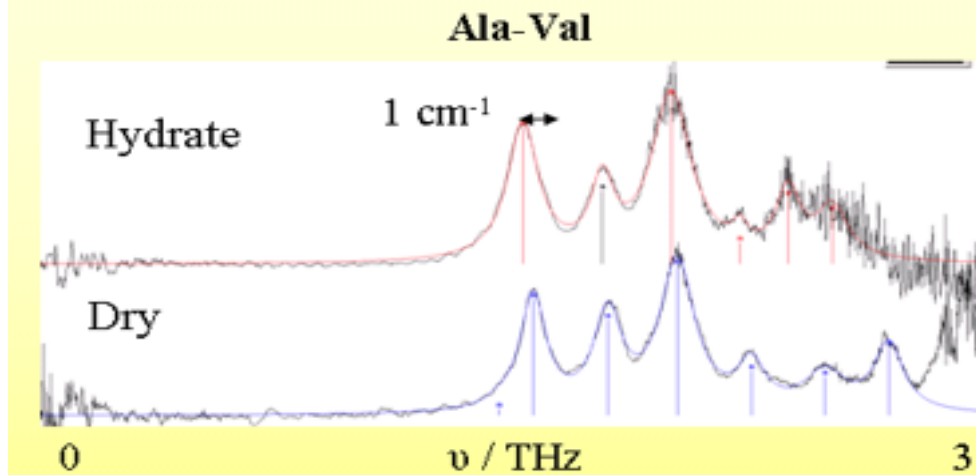


X-ray structures of the parallel (top) and anti-parallel (bottom)  $\beta$ -sheet forms of trialanine.



THz spectra of three crystalline forms of Ala<sub>3</sub>. All three are unique and illustrate the sensitivity in this region to changes in the  $\beta$ -sheet form and the co-crystallized water weakly bound in the lattice.

# Dipeptide nanotubes: Ala-Val & Val-Ala



THz spectra of AV and its retro-analog, VA. The two spectra in each panel were obtained for dehydrated samples (blue) and for samples where water is present in the hydrophobic core region (red)

K. Siegrist and D.F. Plusquellic, NIST Web Site (in prep)

# Vibrational Circular Dichroism: VCD

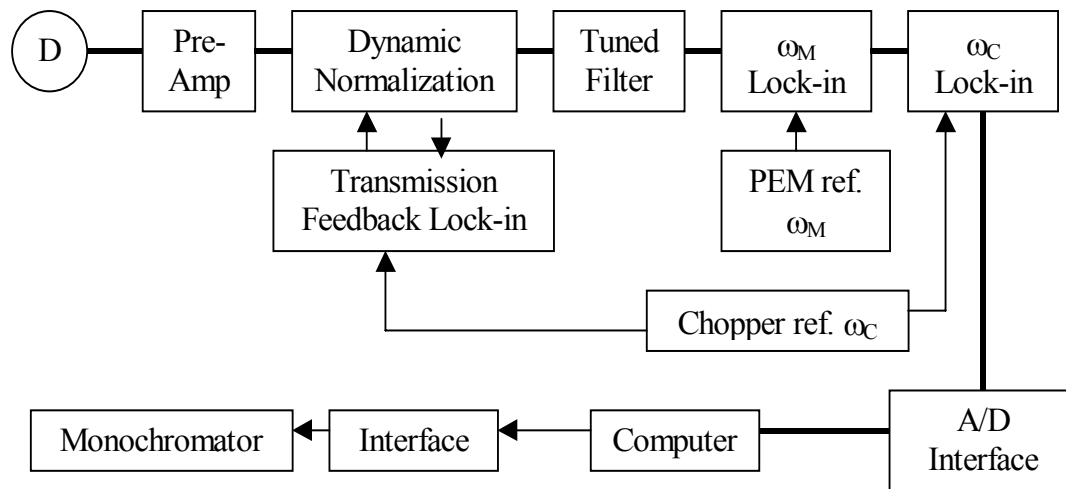
Builds on long tradition of Circular Dichroism (CD) studies in the UV, which still have a large impact on Biomolecular research—comparisons are useful

Combine inherent resolution of vibrational spectra with conformational sensitivity of CD

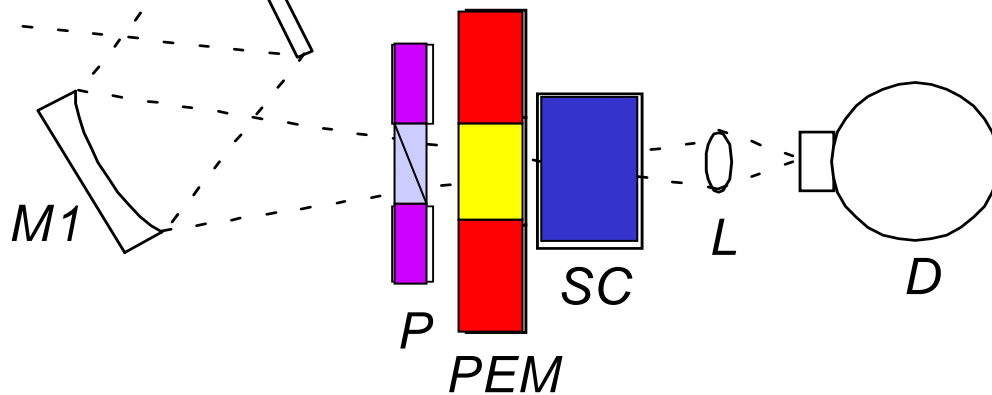
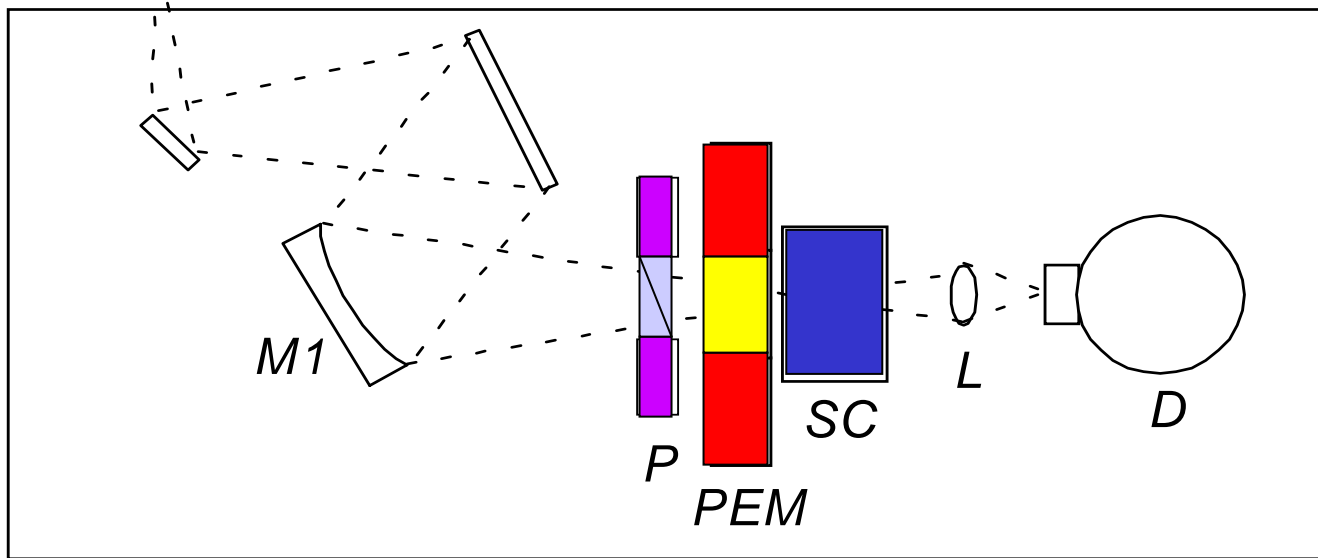
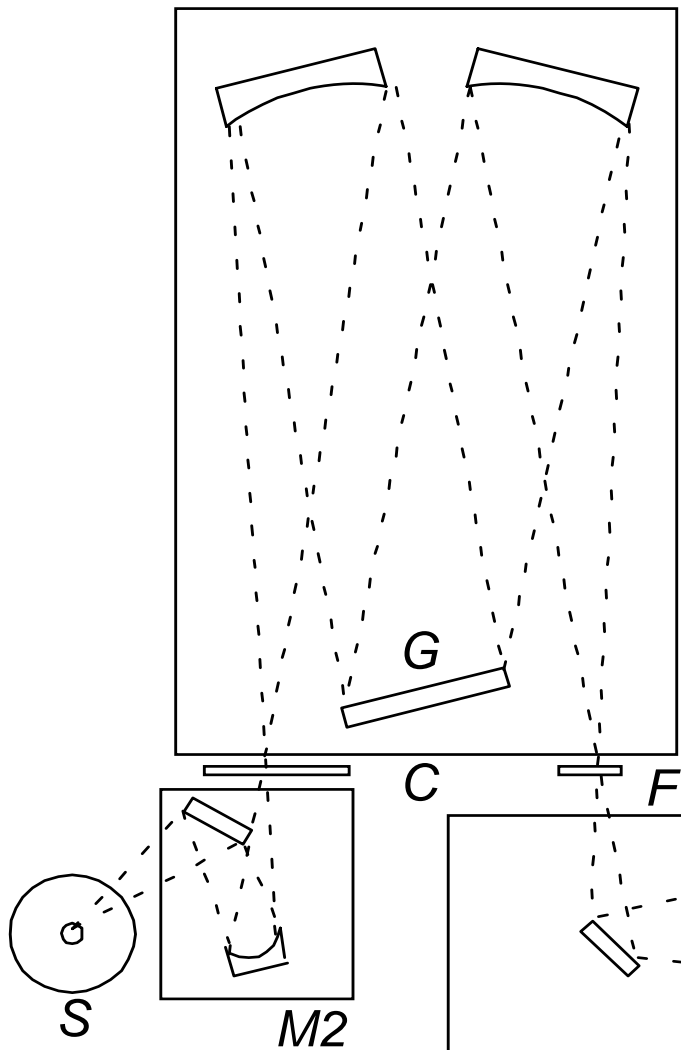
# UIC Dispersive VCD Schematic

Yes it still exists and measures VCD!

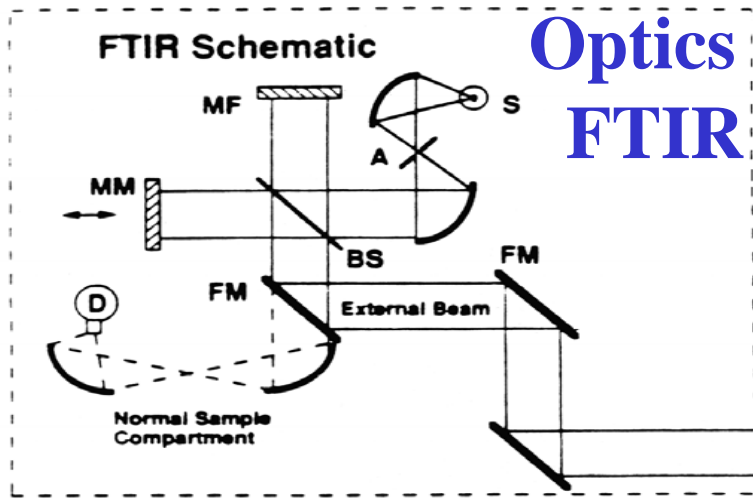
## Electronics



## Optics and Sampling

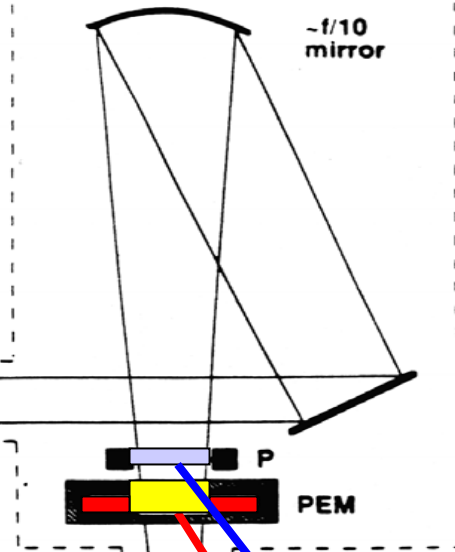






**Optics  
FTIR**

Separate VCD Bench



**UIC  
FT-VCD  
Schematic**

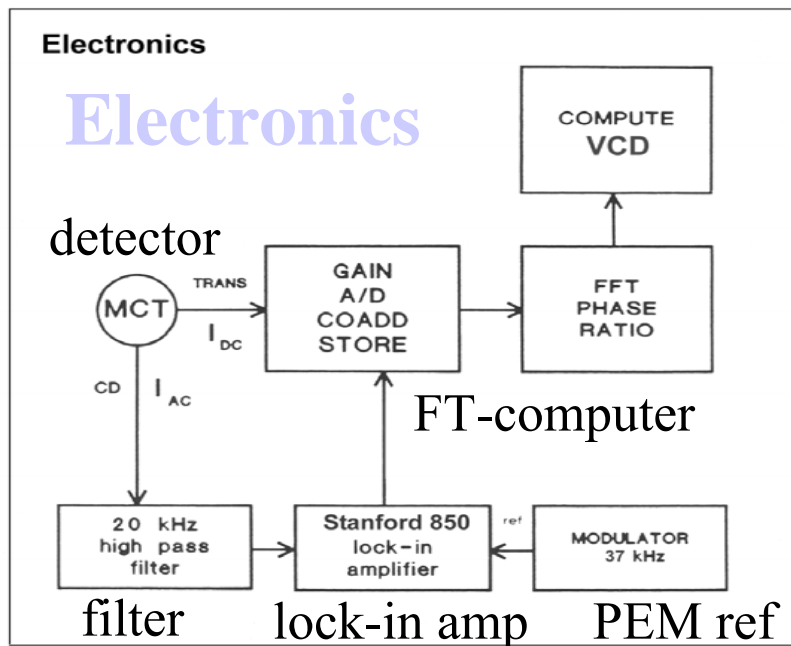
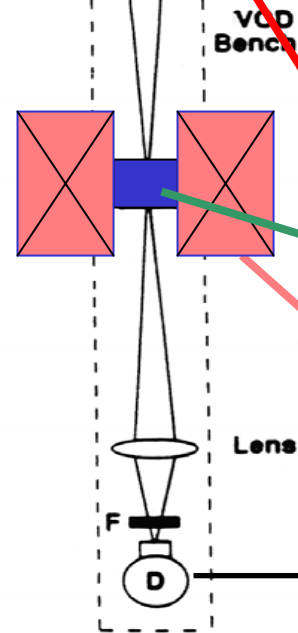
(designed for magnetic VCD  
*commercial ones simpler*)

**Polarizer**

**PEM (ZnSe)**

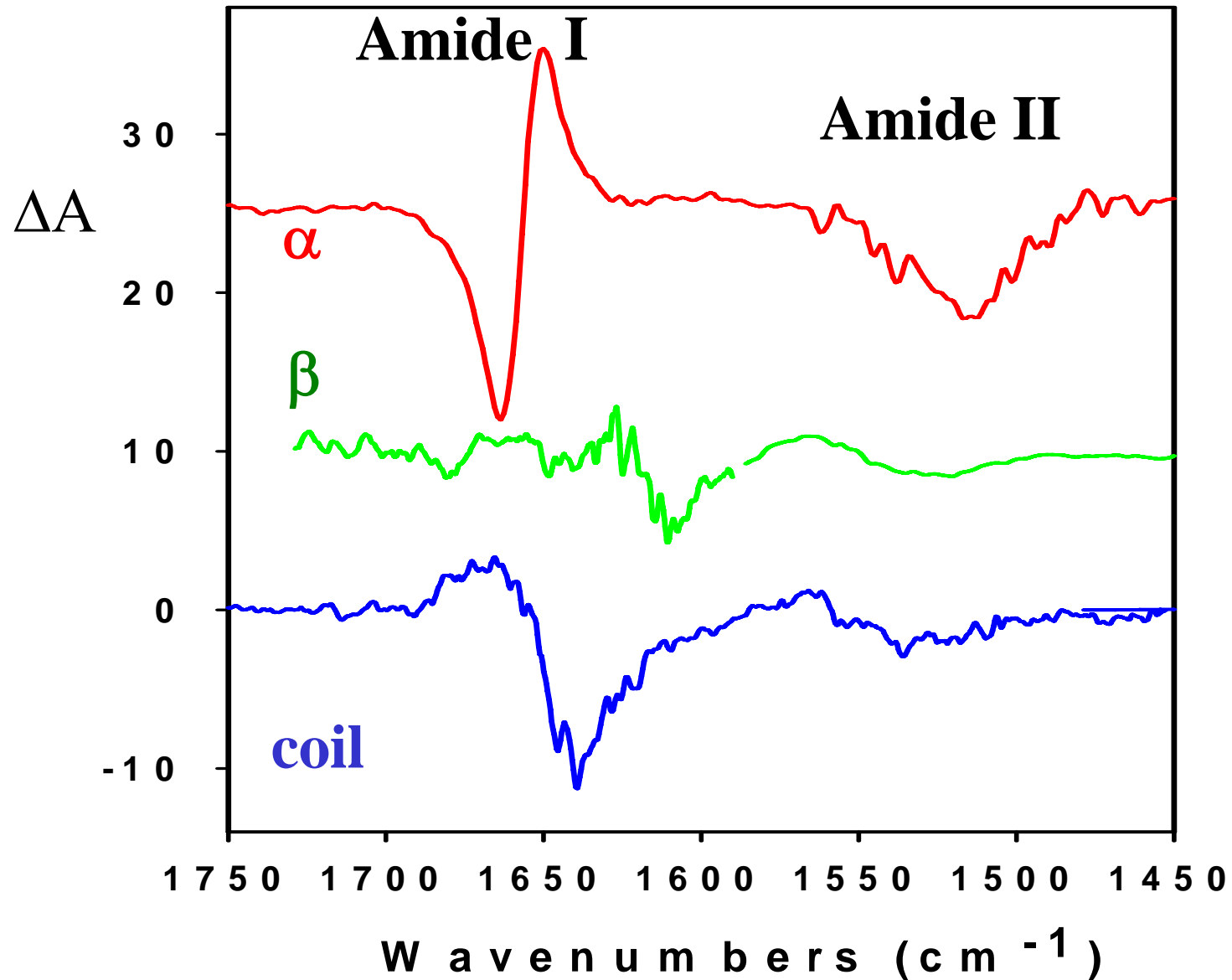
**Sample**

**Optional magnet**

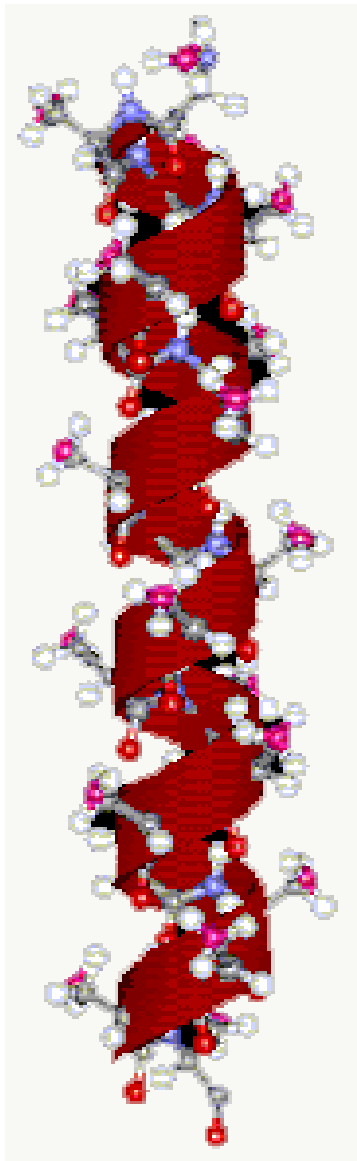




# Selected model Peptide VCD, aqueous solution



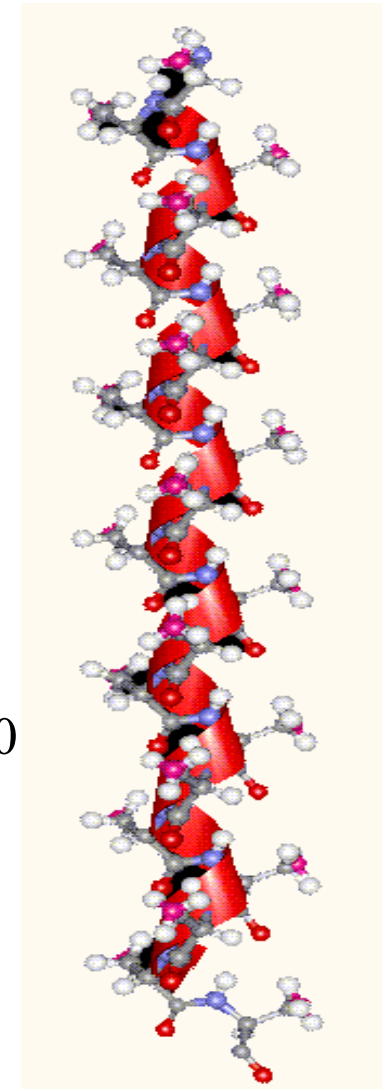
# VCD Example: $\alpha$ - vs. the $3_{10}$ -Helix



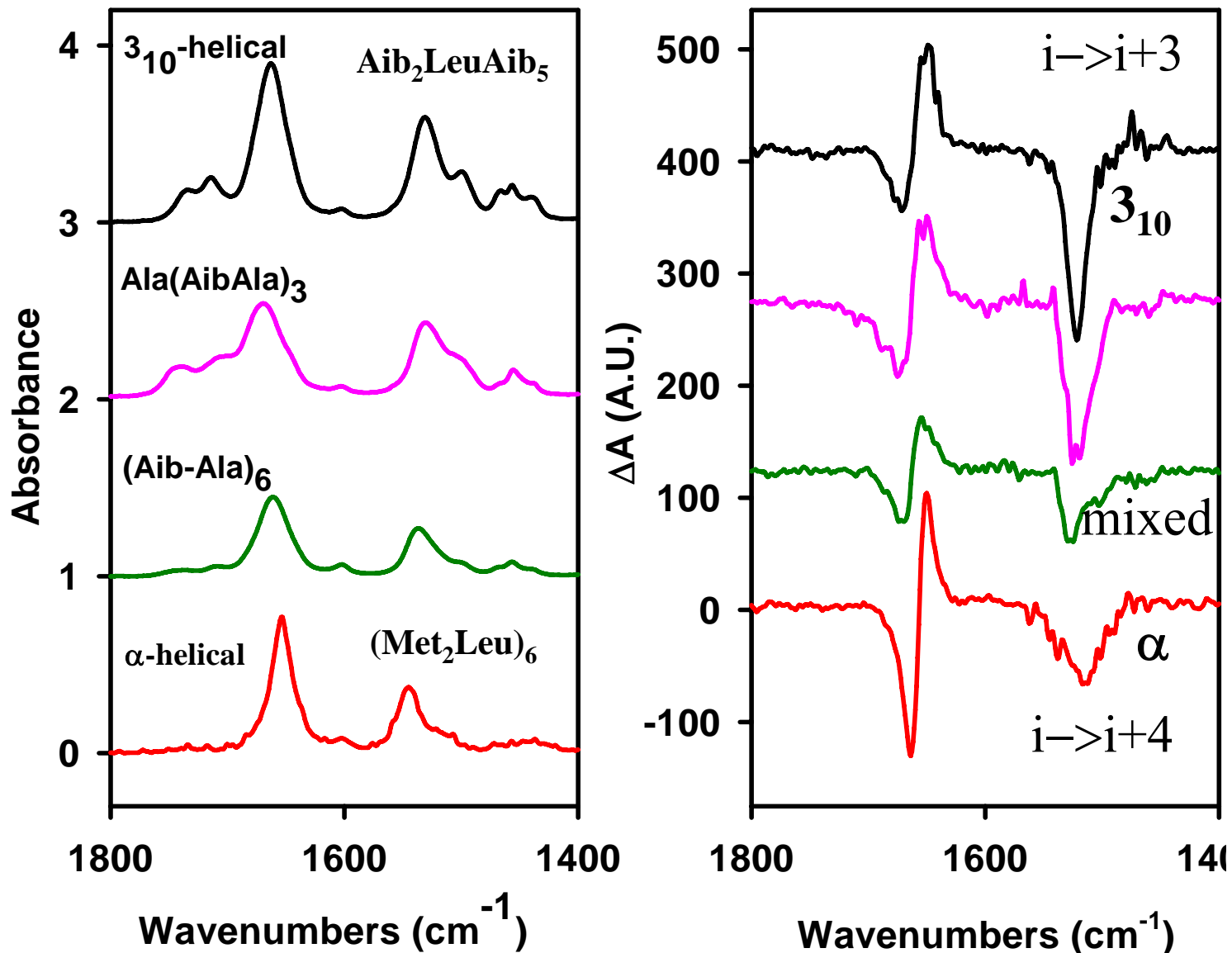
$i+4 \leftarrow$  H-bonding  $\rightarrow i, i+3$

3.6  $\leftarrow$  Res./Turn  $\rightarrow$  3.0

1.00  $\leftarrow$  Trans./Res ( $\text{\AA}$ )  $\rightarrow$  1.50

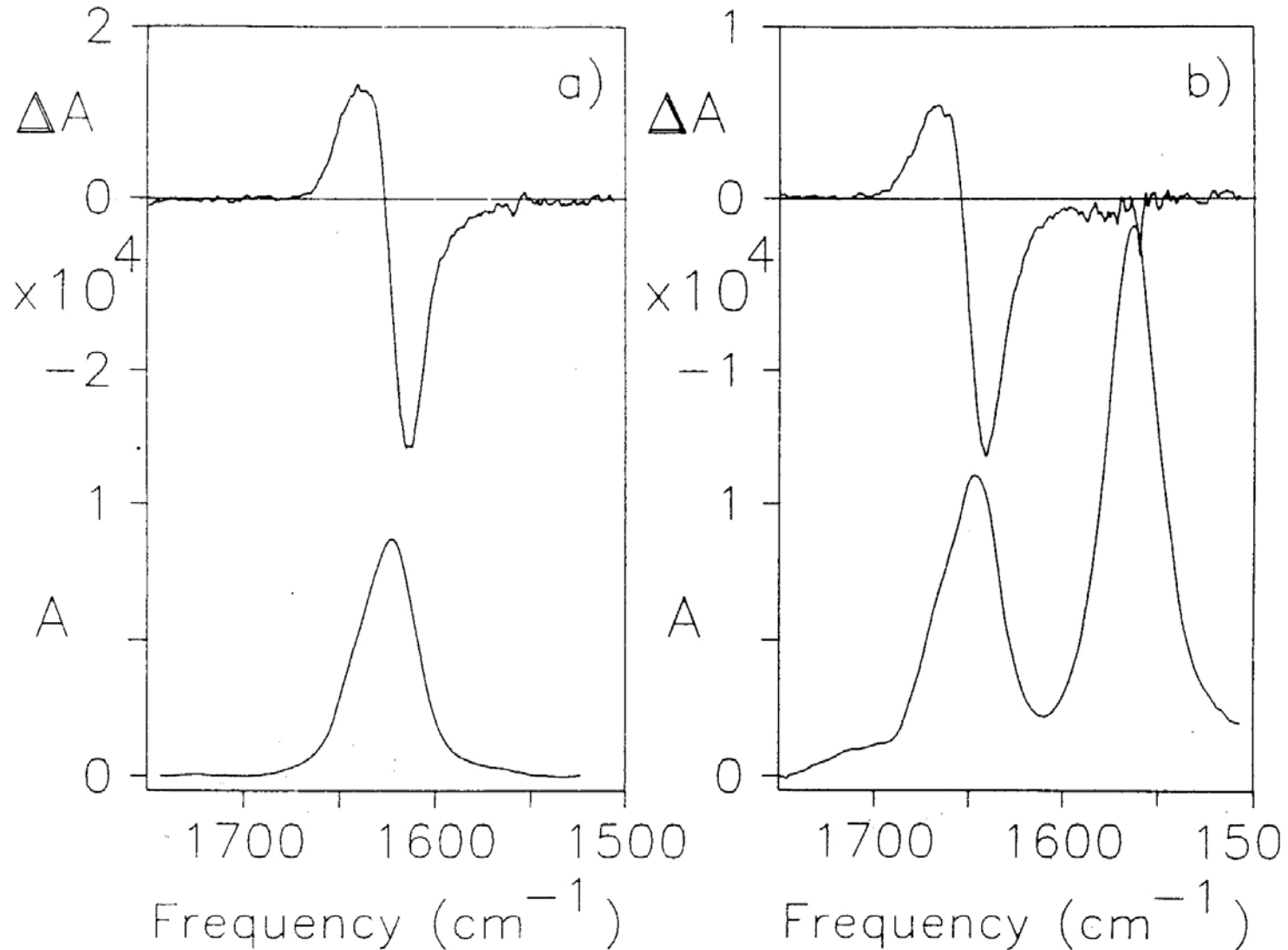


# The VCD success example: $3_{10}$ -helix vs. $\alpha$ -helix



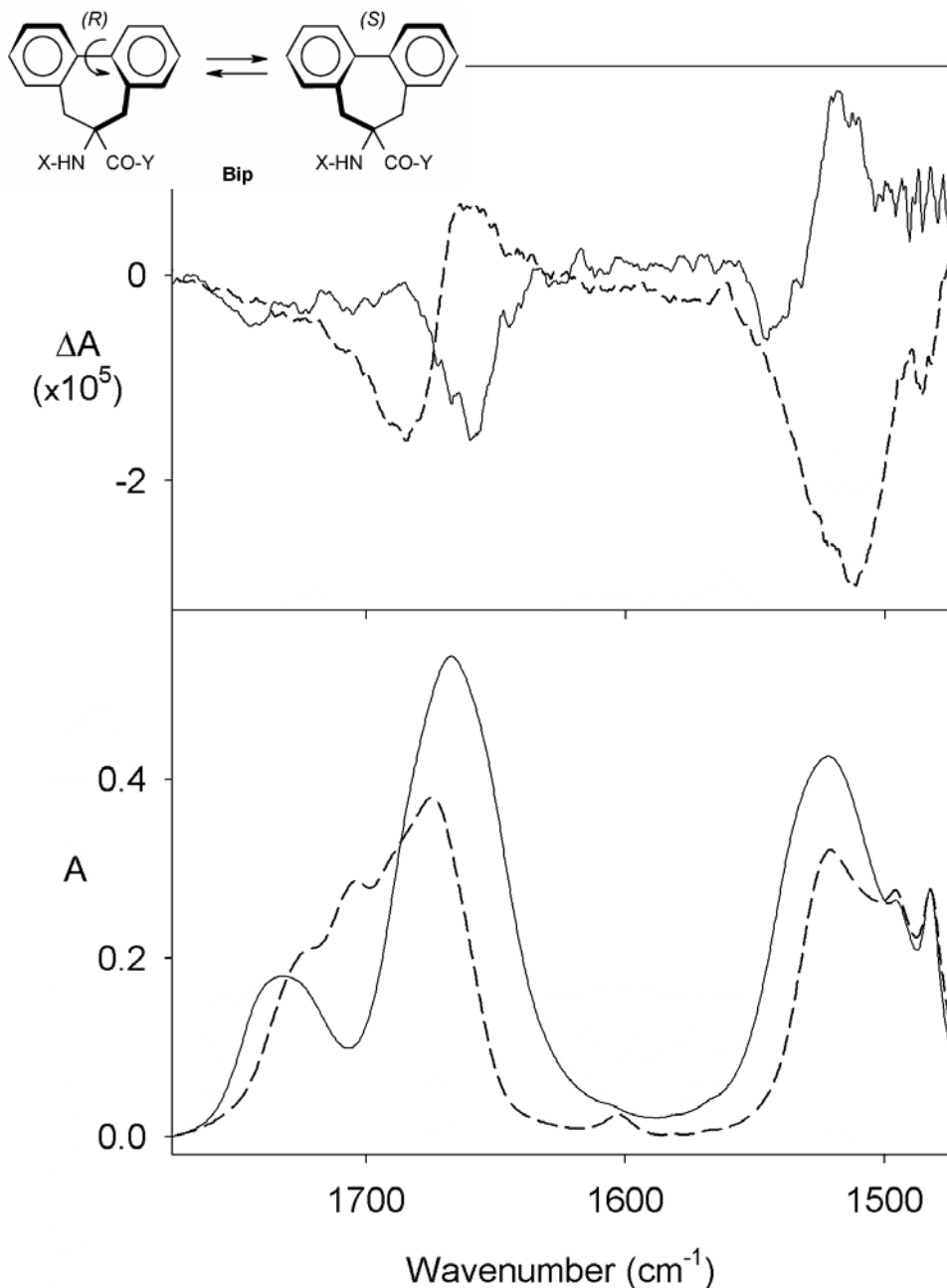
Relative shapes of multiple bands distinguish these similar helices

# Relationship to “random coil” - compare $\text{Pro}_n$ and $\text{Glu}_n$



**IR ~ same, VCD - same shape, half size -- partially ordered**

# Biphenyl bridged residues (Bip) show inversion



Ac-(Bip)<sub>3</sub>-L-Val-OMe (————)

**left-handed**

Boc-L-Val-(Bip)<sub>4</sub>-OtBu (-----)

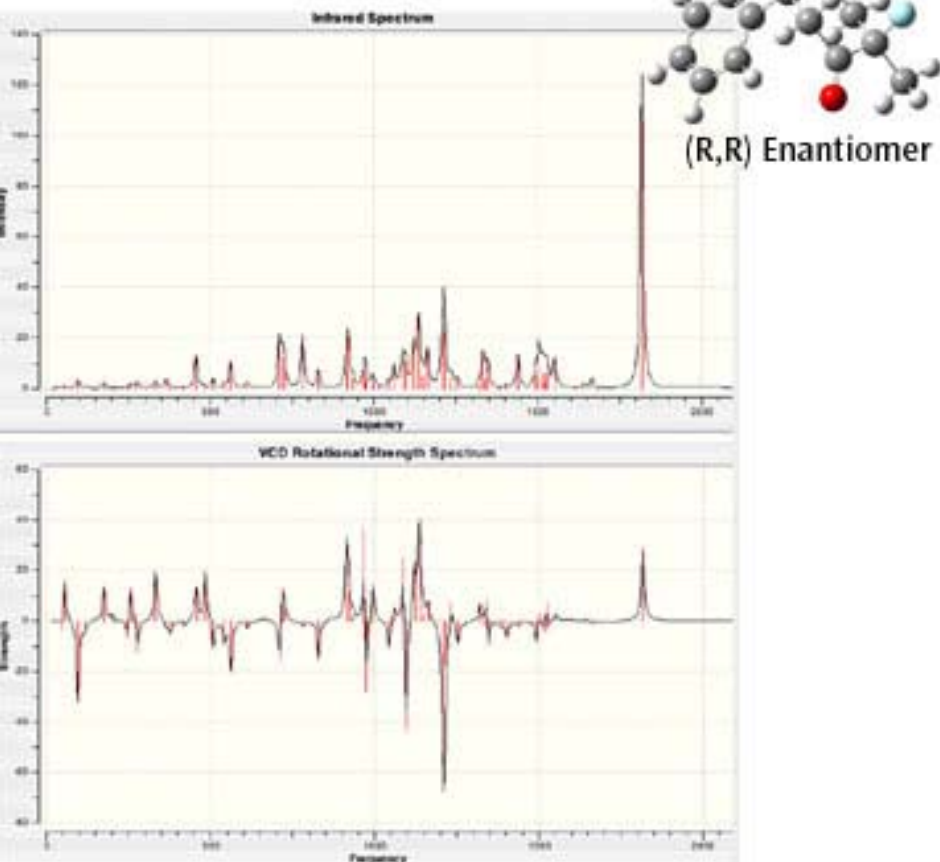
**right-handed (3<sub>10</sub>-helix)**

Vibrational spectrum separates aromatic and amide transitions

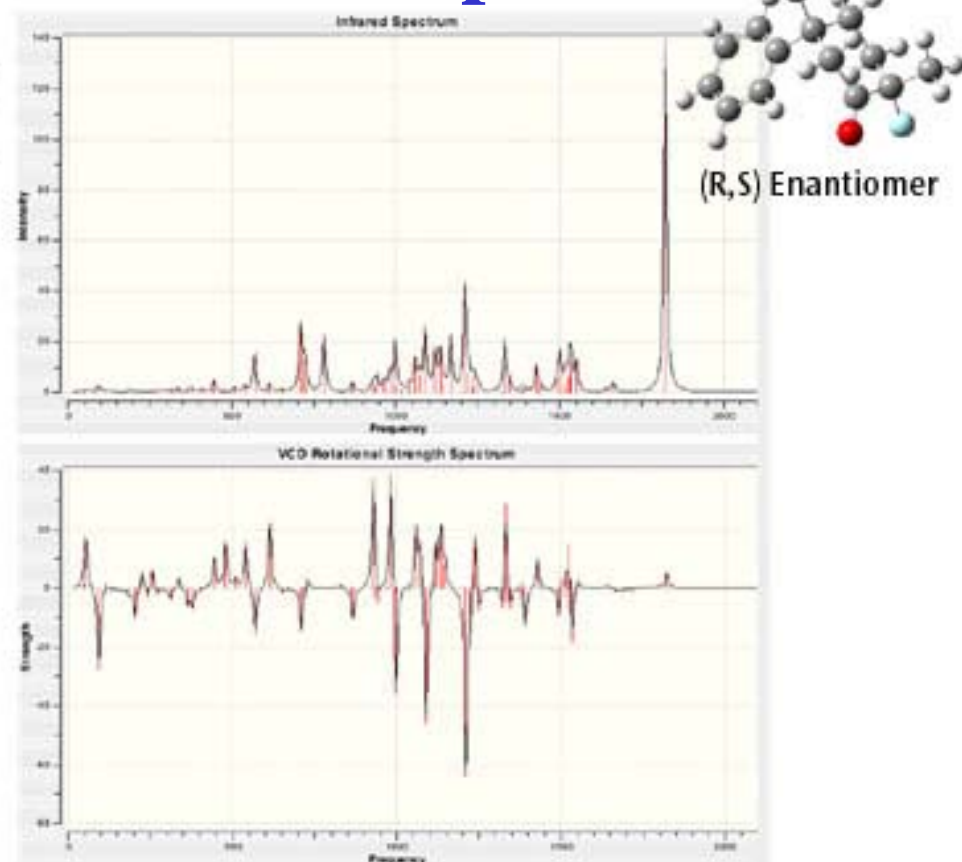
**Figure 1** VCD (upper frame) and IR absorption (lower frame) spectra of Ac-(Bip)<sub>3</sub>-L-Val-OMe (full lines) and Boc-L-Val-(Bip)<sub>4</sub>-OtBu (dashed lines). Spectra of Ac-(Bip)<sub>3</sub>-L-Val-OMe were measured in 46/11 (v/v) CDCl<sub>3</sub>/TFE-OH and Boc-L-Val-(Bip)<sub>4</sub>-OtBu in CDCl<sub>3</sub> solution using the cell pathlength 500  $\mu$ m and peptide concentration of 9.5 and 8.6 g/L, respectively.

Toniolo, co-workers JACS 2004

# Theoretical IR

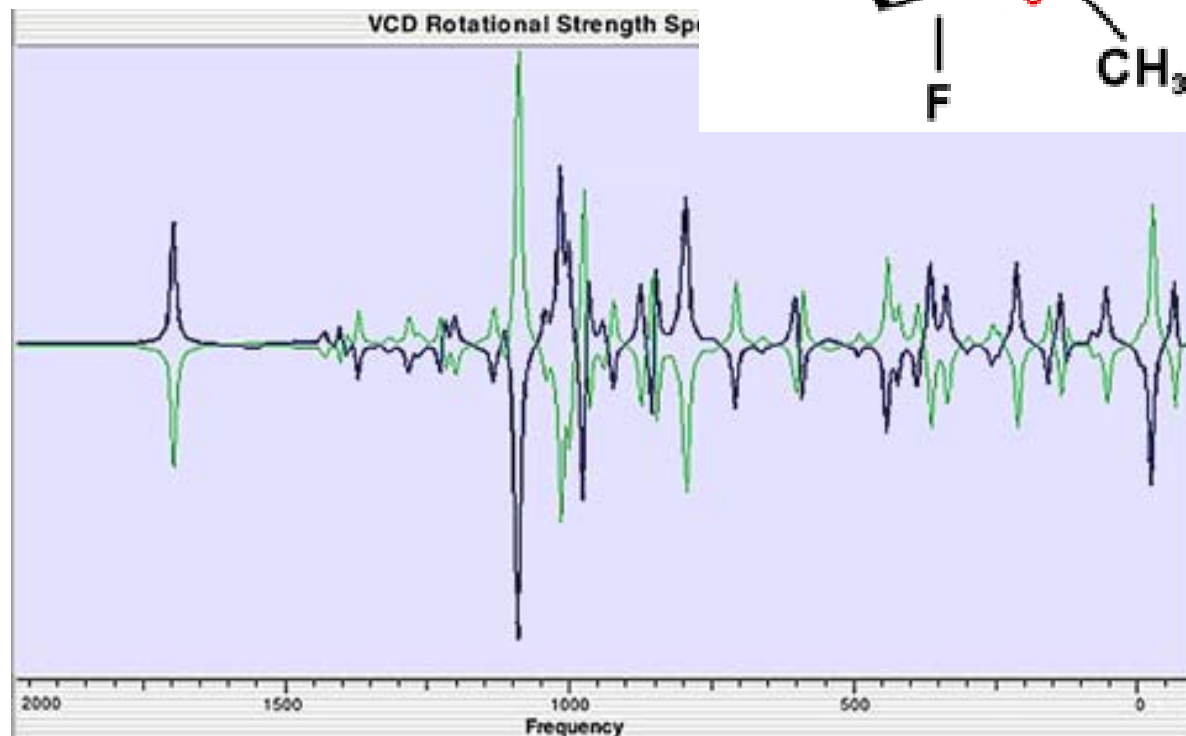
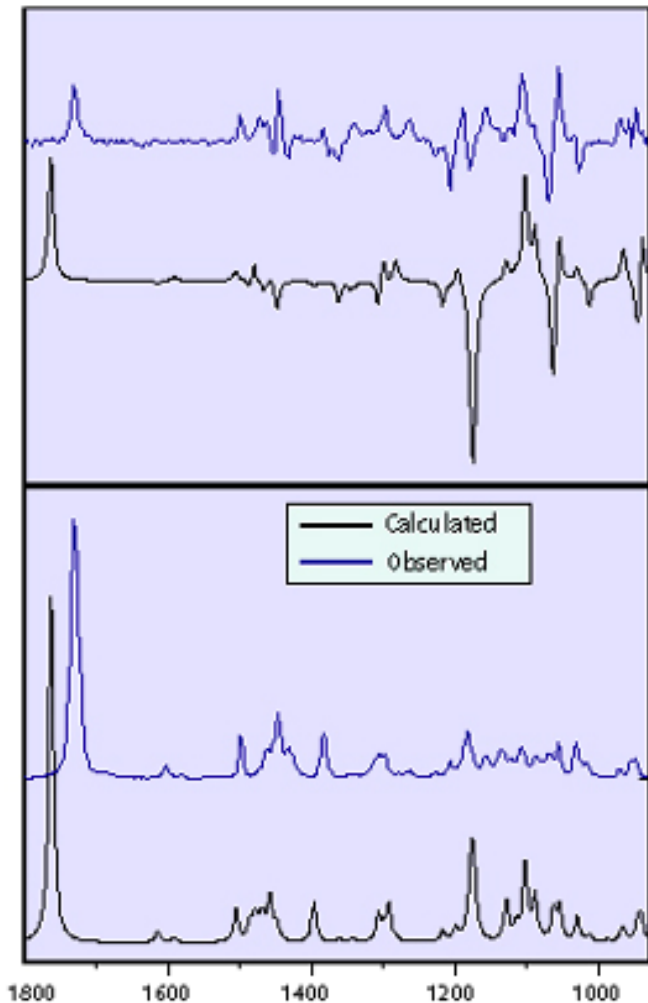
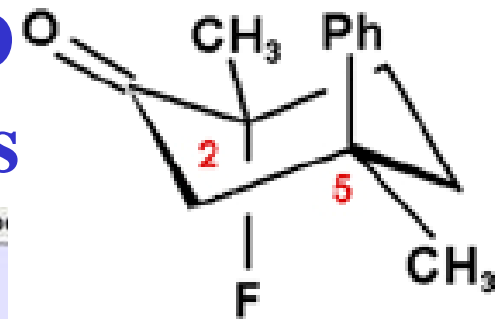


# and VCD spectra



*The predicted IR and VCD spectra for the (R,R) and (R,S) enantiomers. IR spectra are similar, with small differences. The VCD spectra are clearly different. All spectra are truncated at 2100 cm<sup>-1</sup> (there are additional peaks in the 3000-3300 range)*

# Fluoro-ketone VCD Theoretical analysis

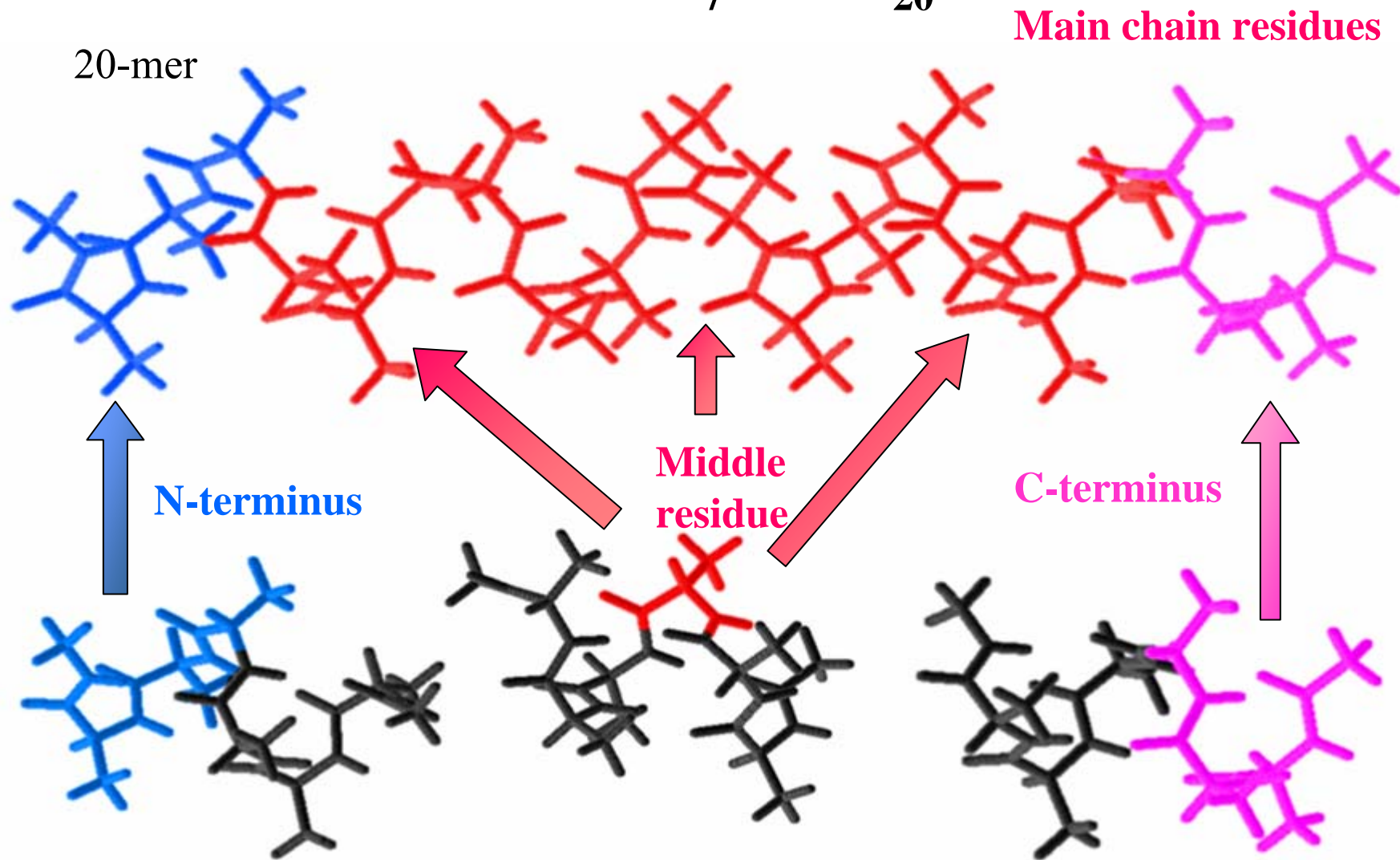


*Comparison of the observed and calculated IR (bottom) and VCD (top) spectra for the (R,R) enantiomer.*

*Predicted VCD spectra for the (R,R) and (S,S) enantiomers (blue and green, respectively).*



# Scheme of the transfer of FF, APT and AAT from Ala<sub>7</sub> to Ala<sub>20</sub>



7-mer: FF, APT, AAT calculated at BPW91/6-31G\* level



# Simulation of Helix IR and VCD Really Works!

**3<sub>10</sub>-helix vs.  $\alpha$ -helix:**

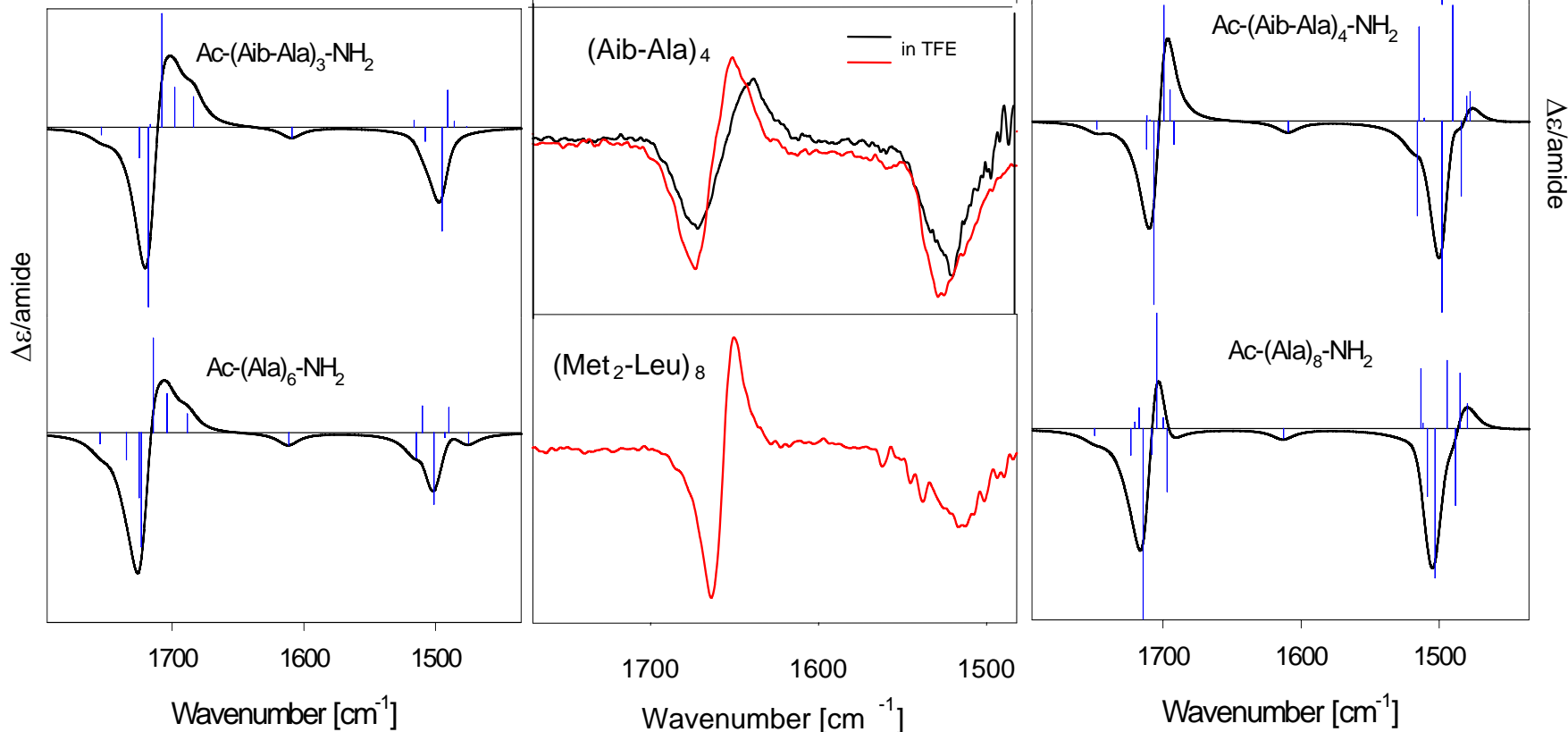
comparison of Aib, Ala and Aib-Ala alternating sequences.

(Kubelka, Silva, Keiderling JACS 2002)

**Experiment:**

**Simulation: 3<sub>10</sub>-helix**

**Simulation:  $\alpha$ -helix**



# Isotope labeling → site specific structure

**Method** - Change  $^{12}\text{C}$  to  $^{13}\text{C}$  on amide  $\text{C}=\text{O}$

Shift frequency down by  $\sim 40 \text{ cm}^{-1}$

Decouple from rest of the chain--test here

**IR** can detect **differences**, but frequencies alone not reliable

**VCD** can determine the **type of secondary structure**

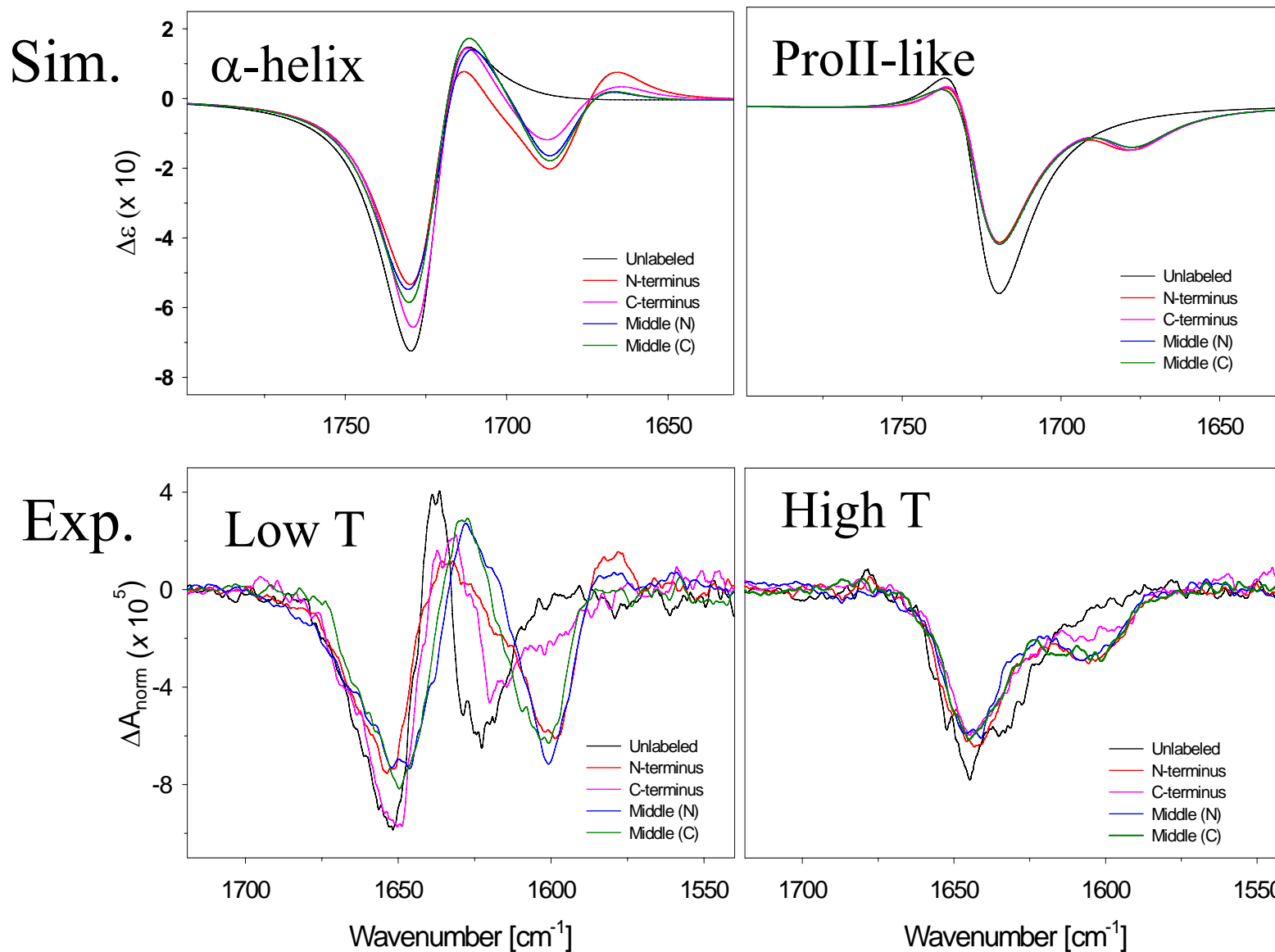
With peptide synthesis, straightforward especially for Ala

**Our studies** coupled Experiment and Theory - **observational**

1.  $\alpha$ -helix thermal denaturation (Silva et al, *PNAS* 2000)
2.  $\beta$ -sheet formation - aggregation (Kubelka & TAK, *JACS* 2001)

# Alanine 20-mer <sup>13</sup>C labeling scheme

Notation	Label position	Peptide sequence
unlabeled	none	Ac-AAAAKAAAKAAAKAAAY-NH <sub>2</sub>
L1	N-terminus	Ac- <u>AAAA</u> KAAAKAAAKAAAY-NH <sub>2</sub>
L2	Middle (closer to N-terminus)	Ac-AAAAK <u>AAAA</u> KAAAKAAAY-NH <sub>2</sub>
L3	Middle (closer to C-terminus)	Ac-AAAAKAAAK <u>AAAA</u> KAAAY-NH <sub>2</sub>
L4	C-terminus	Ac-AAAAKAAAKAAAK <u>AAAY</u> -NH <sub>2</sub>



**Simulated and experimental VCD spectra for labeled Ala<sub>20</sub>**  
 Vary from N- to C terminal, 4 <sup>13</sup>C sequential

Silva, Kubleka, et al. PNAS 2000

# Thanks to you and to SAS!

- Most information is from the literature – thanks to all to those many groups noted
- My students helped get data:
- Rong Huang, Ling Wu, Ning Ge, Ahmed Lakhani, Anjan Roy, Weiyang Zhu, and
- Research Associates: Zhenjia Wang and George Papadonakis
- There is a lot more I cut out - Have a look!.